© 2022. Published by The Company of Biologists Ltd | Development (2022) 149, dev200522. doi:10.1242/dev.200522

RESEARCH ARTICLE

GATA6 is a crucial factor for *Myocd* expression in the visceral smooth muscle cell differentiation program of the murine ureter

Jennifer Kurz[1], Anna-Carina Weiss[1], Timo H.-W. Lüdtke[1], Lena Deuper[1], Mark-Oliver Trowe[1], Hauke Thiesler[2], Herbert Hildebrandt[2], Joerg Heineke[3], Stephen A. Duncan[4] and Andreas Kispert[1,*]

ABSTRACT

Smooth muscle cells (SMCs) are a crucial component of the mesenchymal wall of the ureter, as they account for the efficient removal of the urine from the renal pelvis to the bladder by means of their contractile activity. Here, we show that the zinc-finger transcription factor gene *Gata6* is expressed in mesenchymal precursors of ureteric SMCs under the control of BMP4 signaling. Mice with a conditional loss of *Gata6* in these precursors exhibit a delayed onset and reduced level of SMC differentiation and peristaltic activity, as well as dilatation of the ureter and renal pelvis (hydroureternephrosis) at birth and at postnatal stages. Molecular profiling revealed a delayed and reduced expression of the myogenic driver gene *Myocd*, but the activation of signaling pathways and transcription factors previously implicated in activation of the visceral SMC program in the ureter was unchanged. Additional gain-of-function experiments suggest that GATA6 cooperates with FOXF1 in *Myocd* activation and SMC differentiation, possibly as pioneer and lineage-determining factors, respectively.

KEY WORDS: Ureter, Smooth muscle cell, Differentiation, Mesenchyme, Myocd, Foxf1

INTRODUCTION

In mammals, efficient removal of the urine from the kidneys to the outside relies on the peristaltic activity of a pair of tubular organs: the ureters. Structural basis of the contractile behavior of these straight tubes are smooth muscle cells (SMCs) that form concentric layers in the outer mesenchymal wall. In the mouse, these SMCs arise together with ensheathing fibrocytes in a precisely orchestrated manner from a homogenous pool of mesenchymal progenitors. This pool surrounds the distal aspect of the ureteric bud, an epithelial outgrowth of the nephric duct, at embryonic day (E)11.5. At E12.5, the mesenchymal cells adjacent to the ureteric epithelium (UE) transit from a slender fibroblastic to an enlarged rhomboid shape. At E14.5, they start to express *Myocd*: the key regulator of SMC differentiation (Wang and Olson, 2004). Cells in the direct vicinity of the UE become devoid of *Myocd* expression and differentiate from E16.5 onwards into fibrocytes of the *lamina propria*. The ones further away maintain *Myocd* expression and activate in a stepwise fashion the expression of different SMC structural genes until E18.5. As a consequence, they form a functional *tunica muscularis* that engages in peristaltic activity shortly after the onset of urine production in the fetal kidney at E16.5 (Bohnenpoll et al., 2017a; Bohnenpoll and Kispert, 2014).

Failure to activate the SMC differentiation program in the fetal ureter is detrimental to the integrity of the upper urinary system, i.e. the ureters and kidneys (Bohnenpoll et al., 2017c; Trowe et al., 2012). The urine is no longer propelled to the bladder and therefore accumulates in the ureter and renal pelvis, driving dilatation of these structures that finally results in destruction of the renal parenchyma. Importantly, ureter dilatations are frequently observed in human newborns, and, in most cases, initial dilatation recedes over time. However, in some cases the condition remains unresolved, manifesting as severe uro- and nephropathy (Chiodini et al., 2019; Ek et al., 2007; Herthelius et al., 2020).

A combination of embryological and genetic analyses in the mouse uncovered an interconnected system of signals and transcription factor activities that impinges on the proliferation, patterning and subsequent differentiation of the ureteric mesenchyme (UM) into SMCs and fibrocytes (Bohnenpoll and Kispert, 2014). Sonic hedgehog (SHH) originating from the UE prevents apoptosis in the outer UM, and induces proliferation and SMC differentiation of mesenchymal cells adjacent to the UE. In the latter cells, SHH signaling is required for expression of the transcription factor gene *Foxf1*, which, in turn, induces expression of the gene encoding the signaling molecule BMP4. FOXF1 synergizes in an unknown fashion with BMP4 in activation of *Myocd* expression and SMC differentiation (Bohnenpoll et al., 2017c; Mamo et al., 2017; Yu et al., 2002). WNTs from the UE activate the T-box transcription factors TBX2 and TBX3 to confine the adventitial fate to the outer UM (Aydogdu et al., 2018; Trowe et al., 2012). This could aid in directing the inner UM to the SMC differentiation pathway. Retinoic acid (RA) emanating from the UM and/or the UE delays SMC differentiation possibly by counteracting WNT signaling (Bohnenpoll et al., 2017b).

The GATA transcription factors are a highly conserved family of zinc-finger proteins that mediate tissue-specific gene expression. In mammals there are six family members that based on structure and function were grouped into two subfamilies (Tremblay et al., 2018). We have previously shown that GATA2, a member of the GATA1/2/3 subfamily acts at least partly as a feedback inhibitor of RA signaling to time the activation of *Myocd* and, hence, of SMC differentiation in ureter development (Weiss et al., 2019). Here, we set out to study the functional significance of GATA6, a member of the GATA4/5/6 subfamily, in this process. Of note, GATA6 has been implicated in patterning and differentiation of cardiac neural crest cells into vascular SMCs (Kodo, 2009; Lepore et al., 2006;

[1]Institut für Molekularbiologie, Medizinische Hochschule Hannover, D-30625 Hannover, Germany. [2]Institut für Klinische Biochemie, Medizinische Hochschule Hannover, D-30625 Hannover, Germany. [3]Abteilung für Kardiovaskuläre Physiologie, European Center for Angioscience, Medizinische Fakultät Mannheim, Universität Heidelberg, D-68167 Mannheim, Germany. [4]Department of Regenerative Medicine and Cell Biology, Medical University of South Carolina, Charleston, SC 29425, USA.

*Author for correspondence (kispert.andreas@mh-hannover.de)

J.K., 0000-0002-7382-5789; M.-O.T., 0000-0002-0011-461X; H.H., 0000-0002-1044-0881; J.H., 0000-0002-1541-3030; S.A.D., 0000-0002-2507-7827; A.K., 0000-0002-8154-0257

Handling Editor: Liz Robertson
Received 12 January 2022; Accepted 29 June 2022

Development (2022) 149, dev200522. doi:10.1242/dev.200522

Losa et al., 2017), as well as the maintenance of the quiescent phenotype of these cells (Mano et al., 1999; Perlman et al., 1998; Tremblay et al., 2018). GATA6 is also expressed in bladder SMCs but an *in vivo* requirement for the differentiation of these or other visceral SMCs has not been reported (Kanematsu et al., 2007; Morrisey et al., 1996).

Here, we demonstrate that *Gata6* is expressed in the undifferentiated UM and that its conditional loss from this tissue leads to hydroureternephrosis in fetal and adult mice. Further molecular analyses suggest that GATA6 activates *Myocd* expression and thereby assures timely activation of the SMC differentiation program in the ureter.

RESULTS

Gata6 expression in the undifferentiated UM depends on BMP4 signaling

To obtain a detailed profile of *Gata6* expression in the development of the upper urinary tract, we performed RNA *in situ* hybridization on whole-kidney and ureter rudiments as well as on proximal ureter sections of E11.5 to E18.5 wild-type mouse embryos. Strong *Gata6* expression was found in the entire UM at E11.5 and E12.5. At E14.5 and E16.5, expression at much reduced levels was confined to the inner region of the UM (Fig. 1A,B). *Gata6* expression also occurred in the renal stroma from E12.5 to E18.5 (Fig. S1). GATA6 protein expression in the ureter recapitulated the pattern of *Gata6* mRNA in this organ. The protein was confined to the nucleus at all analyzed stages (Fig. 1C).

To determine whether *Gata6* expression in the UM depends on one of the signaling systems involved in development of this tissue, we analyzed mutants in which key cellular signaling components were conditionally deleted. We used a *Tbx18*^{cre} line, which mediates recombination in the entire UM starting from E11.5 (Airik et al., 2010; Bohnenpoll et al., 2013), and floxed alleles of the unique mediator of SHH signaling, *Smo* (Long et al., 2001), of canonical WNT signaling, *Ctnnb1* (Brault et al., 2001), and of *Bmp4* (Kulessa and Hogan, 2002), as previously reported (Bohnenpoll et al., 2017c; Mamo et al., 2017; Trowe et al., 2012). Loss of *Smo* and *Ctnnb1* had no effect on *Gata6* expression in the UM at E12.5. In contrast, *Gata6* expression was strongly reduced in this region in *Tbx18*$^{cre/+}$; *Bmp4*$^{fl/fl}$ embryos (Fig. 1D). Moreover, in E11.5 kidney rudiments cultured for 18 h with 10 µg/ml of the BMP antagonist noggin (Zimmerman et al., 1996), *Gata6* expression was very weak in the UM, whereas application of 100 ng/ml BMP4 resulted in enhanced and ectopic *Gata6* expression in the renal stroma. Application of 1 µM RA or 1 µM of the pan-RA receptor (RAR) antagonist BMS493 (Chazaud et al., 2003) did not affect *Gata6* expression in this culture system (Fig. 1E). We conclude that expression of *Gata6* in the undifferentiated UM depends on BMP4 signaling.

Loss of *Gata6* in the UM leads to prenatal hydroureter formation

Development of *Gata6*-null embryos arrests during gastrulation as a consequence of defects in extra-embryonic endoderm function (Koutsourakis et al., 1999; Morrisey et al., 1998). We therefore used a conditional gene inactivation approach with a floxed allele of *Gata6* and our *Tbx18*^{cre} line to analyze *Gata6* function specifically in the UM (Airik et al., 2010; Sodhi et al., 2006). The tissue-specific inactivation of *Gata6* in *Tbx18*$^{cre/+}$;*Gata6*$^{fl/fl}$ (*Gata6cKO*) ureters was confirmed by severe downregulation of *Gata6* mRNA in the UM at E11.5 and of GATA6 protein at E12.5 (Fig. S2). In matings of *Tbx18*$^{cre/+}$;*Gata6*$^{fl/+}$ males with *Gata6*$^{fl/fl}$ females, *Gata6cKO* embryos were recovered at the expected ratio at E18.5 and all other analyzed stages (Fig. S3A). The external appearance of E18.5 mutant embryos was normal, but their urogenital system was frequently (~80%) and sex-independently characterized by dilatation of the ureter with the proximal aspect being more affected. The severity of this phenotypic defect ranged from weak unilateral to strong bilateral hydroureter (Fig. 2A, Fig. S3B-E). Testis and epididymis were invariably laterally tethered to the kidney (cryptorchidism) and the adrenals were drastically reduced in size

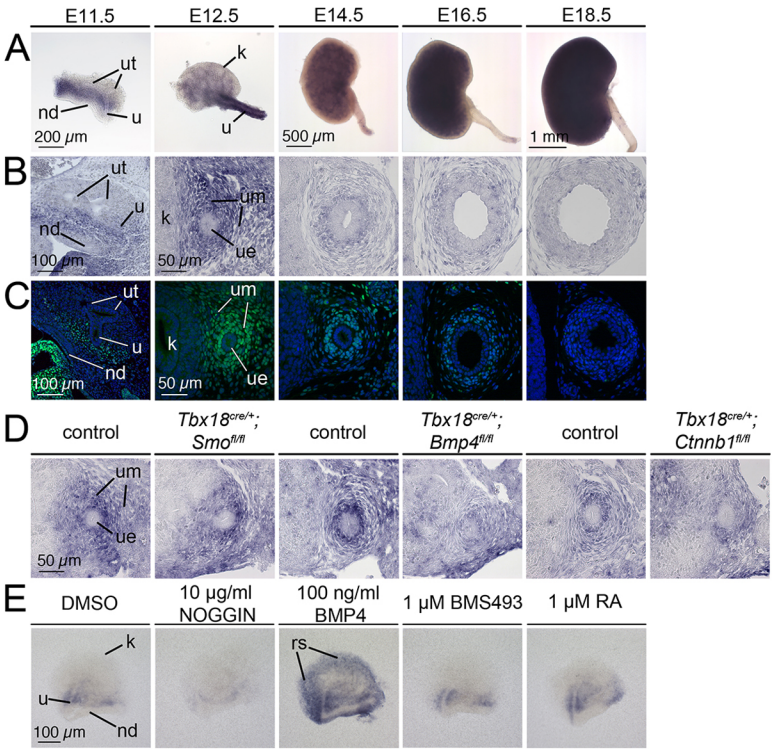

Fig. 1. *Gata6* expression in the undifferentiated mesenchyme of the developing ureter depends on BMP4. (A,B) RNA *in situ* hybridization analysis of *Gata6* expression in whole kidneys and ureters (A), and on sections of the metanephros (E11.5) and of the proximal ureter region (B) derived from E12.5 to E18.5 wild-type embryos. The staining in whole kidneys (A) relates to stromal expression of *Gata6* (see Fig. S1). (C) Immunofluorescence analysis of the GATA6 protein on sections of the metanephric region (E11.5) and of the proximal ureter region of E12.5 to E18.5 wild-type embryos. Nuclei are counterstained with DAPI. (D) RNA *in situ* hybridization analysis of *Gata6* expression on transverse sections through the posterior trunk region of E12.5 control embryos, and of embryos with loss of SHH/SMO signaling (*Tbx18*$^{cre/+}$;*Smo*$^{fl/fl}$), with loss of *Bmp4* (*Tbx18*$^{cre/+}$;*Bmp4*$^{fl/fl}$) and with loss of *Ctnnb1*-dependent WNT signaling (*Tbx18*$^{cre/+}$; *Ctnnb1*$^{fl/fl}$) in the UM. (E) RNA *in situ* hybridization of *Gata6* expression in E11.5 ureter/kidney explants grown for 18 h with DMSO (control), with 10 µg/ml of the BMP4 antagonist noggin, with 100 ng/ml BMP4, with 1 µM of the pan-RAR inhibitor BMS493 or with 1 µM RA. At least three ($n \geq 3$) independent specimens were analyzed for each assay. k, kidney; nd, nephric duct; rs, renal stroma; u, ureter; ue, ureteric epithelium; um, ureteric mesenchyme; ut, ureteric tip.

Development (2022) 149, dev200522. doi:10.1242/dev.200522

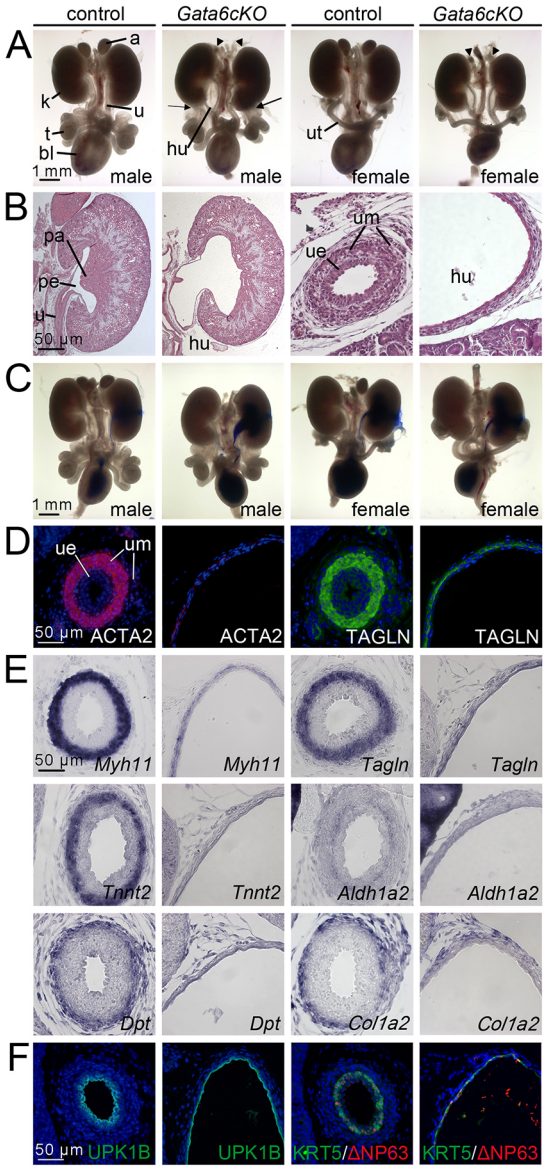

Fig. 2. *Gata6cKO* embryos develop severe hydroureter due to functional insufficiency of the UM at E18.5. (A) Morphology of whole urogenital systems of male and female embryos. Arrows indicate the attachment of the epididymal fat pad to the kidney; arrowheads indicate hypoplastic adrenals in the mutant (control *n*=65; *Gata6cKO* *n*=49). (B) Hematoxylin and Eosin staining on sagittal kidney sections (columns 1 and 2) and transverse sections of the proximal ureter (columns 3 and 4); *n*=3 for each genotype. (C) Analysis of physical obstruction along the ureter and the vesico-ureteric junction by ink injection into the renal pelvis (control, *n*=6; *Gata6cKO*, *n*=5). (D-F) Cyto-differentiation of the UM (D,E) and of the urothelium (F), as shown by immunofluorescence (D,F) and by section RNA *in situ* hybridization analysis (E) of markers. *n*≥3 for each marker per genotype. a, adrenal; bl, bladder; hu, hydroureter; k, kidney; pa, papilla; pe, pelvis; u, ureter; ue, ureteric epithelium; um, ureteric mesenchyme; ut, uterus; t, testis.

(Fig. 2A). The latter phenotype is likely to relate to the reported requirement of *Gata6* in adrenogonadal progenitors (Tevosian et al., 2015), in which *Tbx18*^{cre} also mediates recombination (Häfner et al., 2015). In *Tbx18*$^{cre/+}$;*Gata6*$^{fl/+}$ littermates, the adrenals appeared unchanged, the testis was descended but weak hydroureter formation occurred sex independently in ∼60% of the cases (Fig. S3B-E), indicating a certain degree of haploinsufficiency.

Histological analysis showed that in E18.5 *Gata6cKO* embryos, hydroureter was associated with a dilation of the renal pelvis and a reduction of the renal papilla (Fig. 2B). To exclude the possibility that ureter dilatation is caused or contributed by physical obstruction along the ureter and/or of the vesico-ureteric junction, we injected ink into the renal pelvis and observed its flow upon mild hydrostatic pressure. In all mutants, the ink drained smoothly into the bladder, indicating that a functional rather than a physical obstruction underlies the hydroureteronephrosis (Fig. 2C). To further test this hypothesis, we analyzed proximal ureter sections of E18.5 *Gata6cKO* embryos for presence of SMCs. Markers of this differentiated cell type (ACTA2, TAGLN, *Tagln, Tnnt2* and *Myh11*) were severely downregulated, as was *Aldh1a2*, a marker for fibrocytes of the inner *lamina propria*. Markers for adventitial fibrocytes (*Dpt* and *Col1a2*) were still expressed in the outer loose mesenchyme, albeit more weakly (Fig. 2D,E). Mesenchymal defects did not affect cyto-differentiation of the urothelium, as revealed by normal expression of KRT5, ΔNP63 and UPK1B, which combinatorially mark B cells (KRT5^{+}ΔNP63^{+}UPK1B^{-}), I cells (KRT5^{-}ΔNP63^{+}UPK1B^{+}) and S cells (KRT5^{-}ΔNP63^{-}UPK1B^{+}) (Bohnenpoll et al., 2017a) (Fig. 2F). As increased hydrostatic pressure affects cyto-differentiation in the mesenchymal compartment, we also analyzed weakly dilated proximal ureters and non-dilated distal ureters. Expression of SMC markers was also reduced in these settings but the degree of reduction varied from very strong (*Tnnt2*, ACTA2 and TAGLN) to moderate (*Tagln* and *Myh11*). Fibrocyte and epithelial cyto-differentiation was unaffected (Figs S4,S5). We therefore conclude that SMC differentiation is reduced in E18.5 *Gata6cKO* ureters and that pressure-mediated dilatation aggravates the effect.

Gata6cKO mice do not resolve hydroureter in adolescence

As hydroureter formation is frequently observed in newborn babies but often resolves for unknown reasons (Dudley et al., 1997), we wondered whether the dilative nephro-/uropathy in *Gata6cKO* mice persists into postnatal (P) stages. To answer this question, we analyzed urogenital systems of *Gata6cKO* mice at P21, when the animals showed a normal external appearance and behavior. We found undescended testes, a strongly dilated ureter and pelvis, absence of the renal papilla, and a severe reduction of the renal parenchyma (Fig. 3A-C). Expression of SMC markers was strongly reduced, whereas urothelial differentiation appeared unaffected (Fig. 3D-J). This shows that hydroureternephrosis does not resolve after birth in *Gata6cKO* animals.

Gata6 is required for timely activation of the SMC program

To define both the onset and progression of urogenital malformations in *Gata6cKO* embryos, we analyzed urogenital systems at E14.5 to E16.5, i.e. shortly before and after onset of urine production in the kidney. At the morphological level, the mutant was distinguished by adrenal hypoplasia starting from E14.5, and by hydroureter formation and absent testicular descent at E16.5 (Fig. 4A). Histological staining of proximal ureter sections revealed a less condensed inner mesenchymal layer compared with the control at E15.5, and a strongly dilated ureter at E16.5 (Fig. 4B). In control embryos, expression of *Myh11* started robustly at E14.5, and expression of *Tagln*, *Tnnt2* and ACTA2 started at E15.5 in the UM. In *Gata6cKO* ureters, expression of SMC structural genes/proteins occurred at dramatically reduced levels at all stages analyzed (Fig. 4C,D). In contrast, markers for the *lamina propria* (*Aldh1a2*) and the *tunica adventitia* (*Dpt*, *Fbln2* and *Col1a2*) were either not expressed or were unchanged (Fig. S6). Expression of the epithelial cyto-differentiation markers ΔNP63, UPK1B and KRT5 occurred

Development (2022) 149, dev200522. doi:10.1242/dev.200522

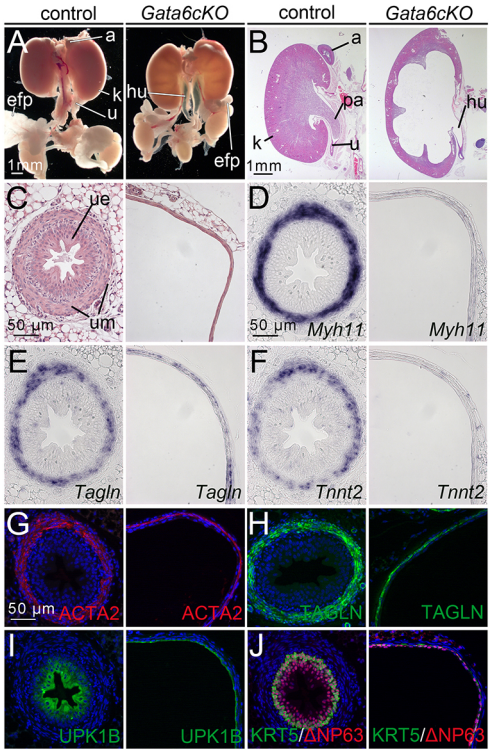

Fig. 3. *Gata6cKO* mice exhibit severe hydroureternephrosis at P21. (A) Morphology of whole urogenital systems of male mice (control *n*=7, mutant *n*=7). Note the attachment of the epididymal fat pad to the kidney, the lack of adrenals and the presence of hydroureter (hu) in the mutant. (B,C) Hematoxylin and Eosin staining on sagittal kidney sections (B) and transverse sections of the proximal ureter (C). (D-H) Analysis of expression of SMC markers on transverse sections of the proximal ureter region by *in situ* hybridization (D-F) and by immunofluorescence (G,H) reveals reduced SMC differentiation in the mutant. (I,J) Analysis of urothelial differentiation by (co-)immunofluorescent detection of the S-cell marker UPK1B (I) and the B-cell marker KRT5 with the I/B-cell marker ΔNP63 (J). (G-J) Nuclei are counterstained with DAPI. *n*≥3 for each marker, genotype and assay (B-J). a, adrenal; hu, hydroureter; efp, epididymal fat pad; k, kidney; pa, papilla; u, ureter; ue, ureteric epithelium; um, ureteric mesenchyme.

normally, but expression of ΔNP63 (at E14.5 and E15.5) and of UPK1B (E15.5) was weaker, and stratification was delayed in *Gata6cKO* ureters (Fig. 4E).

The TUNEL assay did not detect apoptotic bodies in the mutant UM at E12.5 and E14.5 (Fig. S7A). Moreover, cell proliferation, as studied by the BrdU incorporation assay, was not changed in the mesenchymal and epithelial compartments of the mutant ureter at either stage (Fig. S7B,C; Table S1). Hence, *Gata6* is crucial for the initiation of the SMC program but does not affect survival, proliferation and patterning of the UM.

Peristalsis and SMC differentiation occur in a delayed and reduced fashion in *Gata6cKO* ureters

Although SMC differentiation was dramatically reduced in *Gata6cKO* ureters at E14.5 and E15.5, the program may be compromised from E16.5 onwards by pressure-induced ureter dilatation. To analyze ureter development in the absence of urine load, we explanted ureters at E14.5, i.e. before urine formation, and cultured them for 8 days in medium with 10% FCS, monitoring daily for morphological changes and peristaltic activity. In the control, peristaltic movements started after 2 days and reached their frequency peak after 6 days. In *Gata6cKO* ureters, contractions started very weakly only after 4 days, exhibited approximately half of the wild-type frequency after 6 days, but reached the control levels after 8 days of culture (Fig. 5A,B; Table S2). The contraction intensity was strongly decreased at day 4 at the proximal, medial and distal positions analyzed, but reached control levels during the following days, except proximally, where it continued to be significantly reduced (Fig. 5C; Table S3). After 6 days of culture, expression of *Myh11* appeared normal; *Tagln*/TAGLN and ACTA2 expression was weakly reduced and *Tnnt2* was strongly reduced in the proximal ureter region (Fig. 5D). When explants of E14.5 ureters with kidneys were cultured for 8 days in serum-free medium, we also observed a delayed onset and a subsequent partial recovery of the peristaltic activity of *Gata6cKO* ureters, indicating that neither the presence of serum nor absence of kidney accounts for either aspect of the changed peristaltic profile (Fig. S8; Table S4).

Dilated ureters explanted from E18.5 *Gata6cKO* embryos regained frequent peristaltic contractions after 2 to 4 days in culture (Fig. 5E,F; Table S5). Contraction intensity was strongly decreased at days 0 and 2. After 4 and 6 days, control levels were observed medially; at the proximal and distal position, the contraction intensity remained strongly and weakly reduced, respectively (Fig. 5G, Table S6). At day 6 of culture, expression of SMC markers appeared unaffected (*Myh11*), weakly (*Tagln*/TAGLN and ACTA2) and strongly reduced (*Tnnt2*) (Fig. 5H).

Components of the ureteric excitation/conduction system were unchanged in E18.5 *Gata6cKO* embryos, as revealed by normal expression of HCN3, a marker for pelvic pacemaker cells (Hurtado et al., 2010), and of KIT, a marker for interstitial Cajal-like cells (David et al., 2005) (Fig. S9).

These data show that expression of most SMC structural genes/proteins is delayed but not permanently lost in *Gata6cKO* ureters, and that SMC differentiation and peristaltic activity can be partly recovered in *ex vivo* culture conditions even after a dilatation has occurred.

Myocd expression is decreased in *Gata6cKO* ureters

To identify in an unbiased fashion the molecular changes that may cause delayed and reduced SMC differentiation in *Gata6cKO* ureters, we performed microarray-based gene expression profiling of E14.5 *Gata6cKO* and control ureters. Using an intensity threshold of 100 and fold changes of at least 2 in the two individual arrays, we detected 61 genes with reduced and 57 genes with increased expression in mutant ureters (Fig. 6A-C; Tables S7, S8).

Functional annotation using the DAVID software tool (Huang da et al., 2009) revealed an enrichment of gene ontology (GO) terms related to ‘neuron’ in the pool of upregulated genes (Table S9) but RNA *in situ* hybridization did not detect changes of expression of selected candidate genes (*Cartpt*, *Nefm*, *Phox2b* and *Hand2*) in E14.5 *Gata6cKO* ureters (Fig. S10A). Interestingly, two genes relating to RA synthesis, *Aldh1a3* (+5.5) and *Aldh1a2* (+2.2) were the most upregulated genes. Targets of RA signaling in the UM (Bohnenpoll et al., 2017b), including *Wt1* (+2.4) and *Ecm1* (+1.6), were also increased (Fig. 6B, Table S7). RNA *in situ* hybridization confirmed increased expression of *Aldh1a2* and *Wt1* in the outer UM, of *Aldh1a3* in the UE, and of *Ecm1* in the inner UM of *Gata6cKO* ureters at E14.5. However, the direct target of RA signaling, *Rarb* (Mendelsohn et al., 1991), appeared unchanged in the UM (Fig. 6D).

Functional annotation revealed an enrichment of GO terms related to ‘epithelial differentiation’ in the pool of downregulated genes (Table S10). Genes associated with these terms included the S-cell markers *Upk1b* (-4.3), *Upk2* (-3.2) and *Upk1a* (-3.0), the

Development (2022) 149, dev200522. doi:10.1242/dev.200522

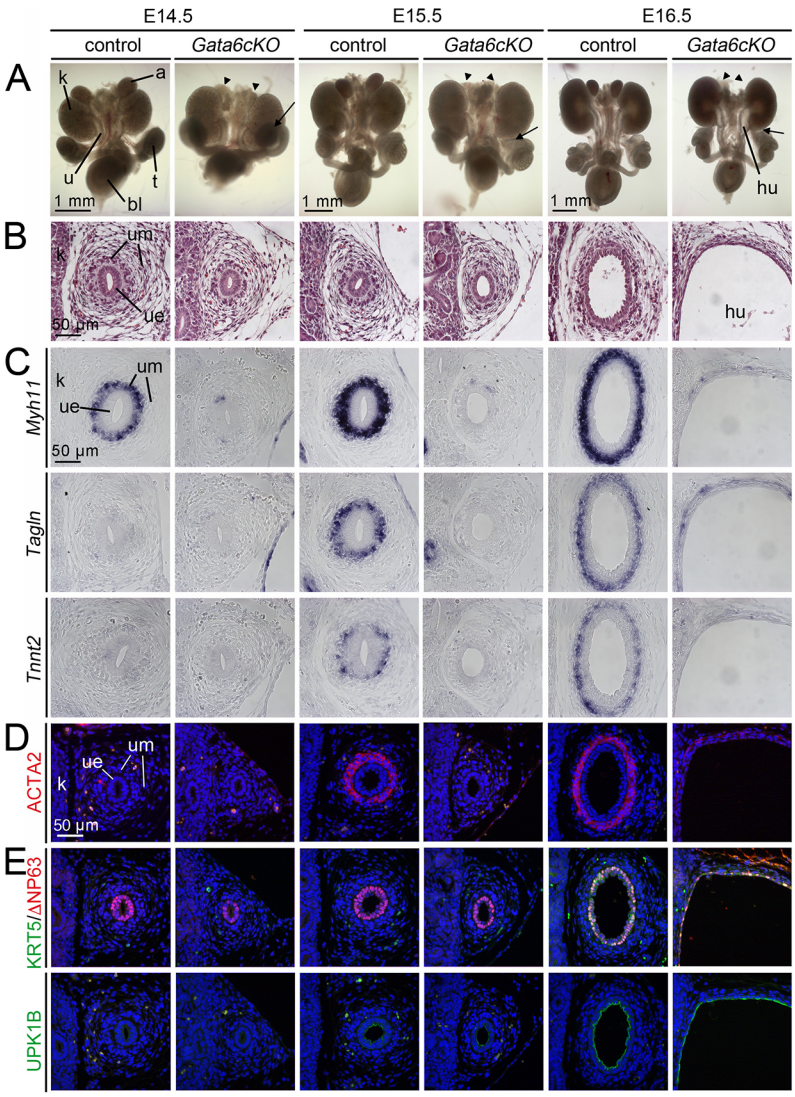

Fig. 4. SMC differentiation is not initiated in *Gata6cKO* ureters at E14.5 to E16.5. (A) Morphology of whole urogenital systems of male embryos. Arrowheads indicate hypoplastic adrenals; arrows indicate undescended testes (E14.5: control, *n*=6; *Gata6cKO*, *n*=7; E15.5: control, *n*=6; *Gata6cKO*, *n*=5; E16.5: control, *n*=24; *Gata6cKO*, *n*=7). (B) Hematoxylin and Eosin staining on transverse sections of the proximal ureter shows hydroureter formation at E16.5, i.e. shortly after onset of urine production in the kidney. (C,D) Expression analysis of SMC markers by RNA *in situ* hybridization on proximal ureter sections (C) and by immunofluorescence (D). (E) Cytodifferentiation of the urothelium, as shown by immunofluorescence for KRT5, ΔNP63 and UPK1B. Nuclei are counterstained with DAPI (D,E). *n*≥3 for each genotype, stage and assay (B-E). a, adrenal gland; bl, bladder; hu, hydroureter; k, kidney; t, testis; u, ureter; ue, ureteric epithelium; um, ureteric mesenchyme.

regulator of S-cell differentiation, *Grhl3* (-2.3) (Yu et al., 2009), and the regulator of epithelial stratification, *Trp63* (-2.5) (Weiss et al., 2013). *In situ* hybridization was not sensitive enough to detect expression changes of these candidate genes in mutant ureters (Fig. S10B). The list of downregulated genes also included *Car3 (-3.2)* and the WNT antagonist *Shisa2* (-3.1), two genes previously shown to be expressed in the UM (Airik et al., 2010; Aydogdu et al., 2018), and most notably *Myocd* (-2.8): the master regulator of SMC differentiation (Wang and Olson, 2004). RNA *in situ* hybridization confirmed reduced expression of *Car3* and *Shisa2* in the UM of E14.5 *Gata6cKO* embryos; *Myocd* expression was almost absent (Fig. 6E).

Myocd expression and SMC differentiation in the developing ureter depends on a number of signaling pathways and transcription factor activities (Bohnenpoll and Kispert, 2014). Our microarray and *in situ* hybridization analyses did not detect changes in expression of *Shh* or of the direct target genes of SHH signaling, *Ptch1* and *Gli1* (Bohnenpoll et al., 2017c; Ingham and McMahon, 2001); of *Wnt7b* and *Wnt9b*; of *Axin2*, a direct target of this pathway (Jho et al., 2002; Trowe et al., 2012); of *Bmp4* (Bohnenpoll et al., 2017c) and the direct targets of its activity, *Id2* and *Id4* (Hollnagel et al., 1999; Mamo et al., 2017); and of the transcription factor genes *Foxf1* (Bohnenpoll et al., 2017c), *Gata2* (Weiss et al., 2019), S*ox9* (Airik et al., 2010), *Tbx18* (Airik et al., 2006), *Tcf21* (Airik et al., 2006), *Tshz*3 (Caubit et al., 2008), *Tbx2/TBX2* and *Tbx3/TBX3* (Aydogdu et al., 2018) in *Gata6cKO* ureters at E14.5 (Figs S11,S12).

RT-qPCR analysis confirmed that *Myocd* expression was strongly reduced in E14.5 *Gata6cKO* ureters, whereas expression of *Foxf1* (an activator of *Myocd* expression), of the WNT target gene *Axin2*, of the BMP4 target *Id2* and of the mesenchymal RA target *Rarb* was unchanged (Fig. 6F, Table S11). Expression of *Myocd* remained strongly reduced at E15.5 and E16.5. In E18.5 ureters and in E18.5 ureter explants cultured for 6 days *Myocd* expression was weakly reduced, indicating that *Myocd* expression is regained to a significant degree after E16.5 (Fig. 6G). Hence, *Gata6* is required for activation of *Myocd* expression at E14.5, independently of transcription factors and signaling activities previously implicated in the regulation of this gene.

Enhanced RA signaling does not account for the peristalsis defects of *Gata6cKO* ureters

Although our assays did not detect increased expression of the direct RA target gene *Rarb* in the UM, increased expression of RA synthesizing enzymes and some RA-dependent genes may point to a functional implication of enhanced RA signaling in the delayed

Development (2022) 149, dev200522. doi:10.1242/dev.200522

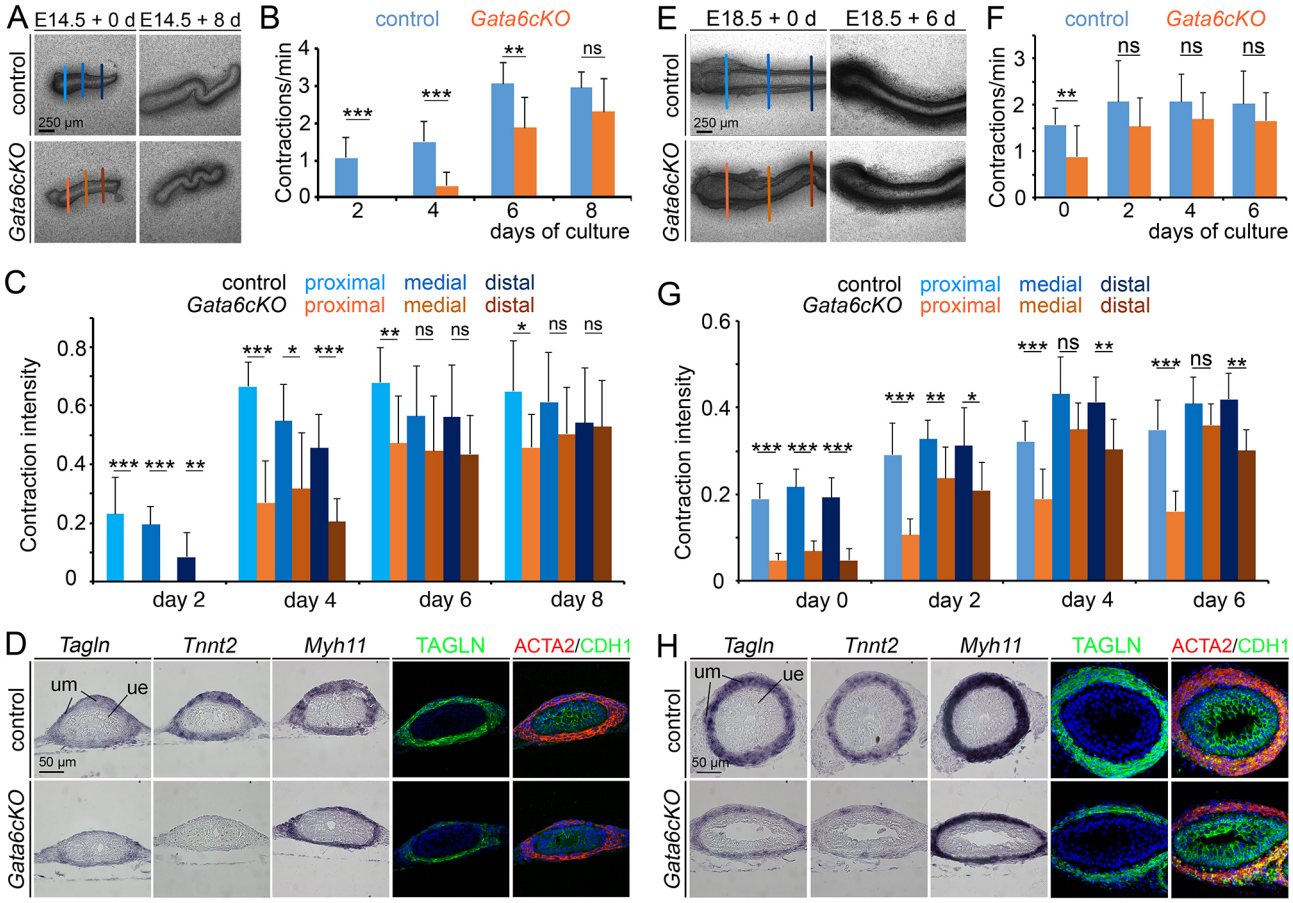

Fig. 5. Peristaltic activity and SMC differentiation are regained *in Gata6cKO* ureters in absence of hydrostatic pressure. (A) E14.5 ureters were explanted and grown for 8 days in culture. Vertical lines indicate proximal, medial and distal ureter levels. Morphology and peristaltic activity were monitored every second day using video microscopy. (B) Statistical analysis of peristaltic activity (expressed as contractions per min) of control (n=8) and mutant ureters (n=8). Data are mean±sd. Differences were considered significant at *P<0.05 , highly significant at **P≤0.005 and extremely significant at ***P≤ 0.0005, two-tailed Student's t-test. For source data and statistics, see Table S2. (C) Analysis of contraction intensity measured at proximal, medial and distal levels of E14.5 ureters. Significance levels are as in B. For source data and statistics, see Table S3. (D) Analysis of SMC differentiation of the UM by RNA *in situ* hybridization and immunofluorescence of markers on sections of explants of E14.5 ureters grown for 6 days in culture. n≥3 for each genotype and probe. (E) E18.5 ureters were explanted and grown for 6 days in culture. Vertical lines indicate proximal, medial and distal ureter levels. (F) Statistical analysis of peristaltic activity (expressed as contractions per min) of control (n=11) and mutant ureters (n=8). Data are mean±sd. Significance levels are as in B. For source data and statistics, see Table S5. (G) Analysis of contraction intensity measured at proximal, medial and distal levels of E18.5 ureters. Significance levels are as in B. For source data and statistics, see Table S6. (H) Analysis of SMC differentiation of the UM by RNA *in situ* hybridization and immunofluorescence of markers on sections of explants of E18.5 ureters grown for 6 days in culture. n≥3 for each genotype and probe. ue, ureteric epithelium; um, ureteric mesenchyme.

onset of SMC differentiation, as previously reported (Bohnenpoll et al., 2017b; Weiss et al., 2019). We therefore tested whether reduction of RA signaling ameliorates the peristaltic changes of *Gata6cKO* ureters. Treatment of control E13.5 ureter explants with the pan-RAR antagonist BMS493 (1 µM) did not affect the onset of contractions but lowered the contraction frequency from day 4 onwards. In *Gata6cKO* ureters, BMS493 treatment further delayed the peristaltic onset and reduced the contraction frequency (Fig. S13; Table S12). We conclude that increased RA signaling does not contribute in a major fashion to the delayed onset of SMC differentiation and peristaltic activity in *Gata6cKO* ureters.

Gata2 and *Gata6* do not cooperate in SMC differentiation in the developing ureter

We recently reported that, in mice with conditional loss of *Gata2* in the UM, SMC differentiation was delayed and RA signaling was increased (Weiss et al., 2019). Given the phenotypic similarities, we wondered whether GATA2 and GATA6 would cooperate in ureteric SMC differentiation. We tested this by generating mice that were compound heterozygous for *Gata2* and *Gata6*. Urogenital systems of $Tbx18^{cre/+}$;$Gata2^{fl/+}$;$Gata6^{fl/+}$ embryos neither exhibited enhanced ureter dilatation nor presented with cryptorchidism compared with $Tbx18^{cre/+}$;$Gata2^{fl/+}$ and $Tbx18^{cre/+}$;$Gata6^{fl/+}$ embryos, indicating that *Gata2* and *Gata6* control different molecular programs (Fig. S14).

GATA6 and FOXF1 cooperate in *Myocd* activation and SMC differentiation

To further analyze the role of GATA6 in *Myocd* activation, we employed a gain-of-function approach in a cellular system. Transfection of a *Gata6* overexpression construct into NIH3T3 cells led to a marginal activation of *Myocd* transcription. In contrast, *Foxf1*, a known regulator of SMC differentiation in the UM (Bohnenpoll et al., 2017c), dose dependently and strongly activated *Myocd* expression in these cells. Intriguingly, co-transfection of *Gata6* and *Foxf1* overexpression constructs activated *Myocd* expression to levels clearly exceeding those achieved with individual transfections (Fig. 7A, Table S13).

Development (2022) 149, dev200522. doi:10.1242/dev.200522

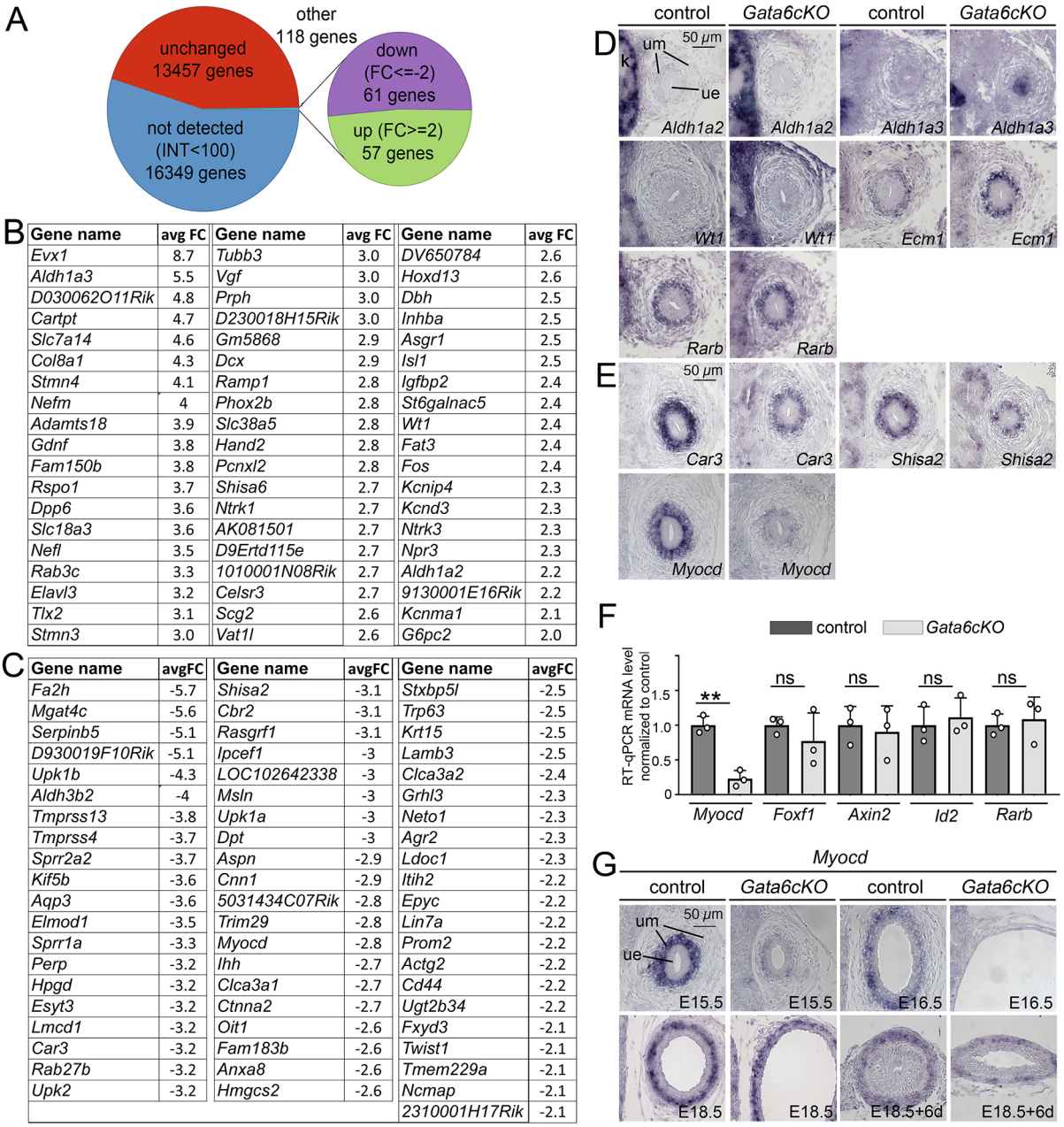

Gene name	avg FC	Gene name	avg FC	Gene name	avg FC
Evx1	8.7	*Tubb3*	3.0	*DV650784*	2.6
Aldh1a3	5.5	*Vgf*	3.0	*Hoxd13*	2.6
D030062O11Rik	4.8	*Prph*	3.0	*Dbh*	2.5
Cartpt	4.7	*D230018H15Rik*	3.0	*Inhba*	2.5
Slc7a14	4.6	*Gm5868*	2.9	*Asgr1*	2.5
Col8a1	4.3	*Dcx*	2.9	*Isl1*	2.5
Stmn4	4.1	*Ramp1*	2.8	*Igfbp2*	2.4
Nefm	4	*Phox2b*	2.8	*St6galnac5*	2.4
Adamts18	3.9	*Slc38a5*	2.8	*Wt1*	2.4
Gdnf	3.8	*Hand2*	2.8	*Fat3*	2.4
Fam150b	3.8	*Pcnxl2*	2.8	*Fos*	2.4
Rspo1	3.7	*Shisa6*	2.7	*Kcnip4*	2.3
Dpp6	3.6	*Ntrk1*	2.7	*Kcnd3*	2.3
Slc18a3	3.6	*AK081501*	2.7	*Ntrk3*	2.3
Nefl	3.5	*D9Ertd115e*	2.7	*Npr3*	2.3
Rab3c	3.3	*1010001N08Rik*	2.7	*Aldh1a2*	2.2
Elavl3	3.2	*Celsr3*	2.7	*9130001E16Rik*	2.2
Tlx2	3.1	*Scg2*	2.6	*Kcnma1*	2.1
Stmn3	3.0	*Vat1l*	2.6	*G6pc2*	2.0

Gene name	avgFC	Gene name	avgFC	Gene name	avgFC
Fa2h	-5.7	*Shisa2*	-3.1	*Stxbp5l*	-2.5
Mgat4c	-5.6	*Cbr2*	-3.1	*Trp63*	-2.5
Serpinb5	-5.1	*Rasgrf1*	-3.1	*Krt15*	-2.5
D930019F10Rik	-5.1	*Ipcef1*	-3	*Lamb3*	-2.5
Upk1b	-4.3	*LOC102642338*	-3	*Clca3a2*	-2.4
Aldh3b2	-4	*Msln*	-3	*Grhl3*	-2.3
Tmprss13	-3.8	*Upk1a*	-3	*Neto1*	-2.3
Tmprss4	-3.7	*Dpt*	-3	*Agr2*	-2.3
Sprr2a2	-3.7	*Aspn*	-2.9	*Ldoc1*	-2.3
Kif5b	-3.6	*Cnn1*	-2.9	*Itih2*	-2.2
Aqp3	-3.6	*5031434C07Rik*	-2.8	*Epyc*	-2.2
Elmod1	-3.5	*Trim29*	-2.8	*Lin7a*	-2.2
Sprr1a	-3.3	*Myocd*	-2.8	*Prom2*	-2.2
Perp	-3.2	*Ihh*	-2.7	*Actg2*	-2.2
Hpgd	-3.2	*Clca3a1*	-2.7	*Cd44*	-2.2
Esyt3	-3.2	*Ctnna2*	-2.7	*Ugt2b34*	-2.2
Lmcd1	-3.2	*Oit1*	-2.6	*Fxyd3*	-2.1
Car3	-3.2	*Fam183b*	-2.6	*Twist1*	-2.1
Rab27b	-3.2	*Anxa8*	-2.6	*Tmem229a*	-2.1
Upk2	-3.2	*Hmgcs2*	-2.6	*Ncmap*	-2.1
				2310001H17Rik	-2.1

Fig. 6. Expression of *Myocd* is delayed and reduced in *Gata6cKO* ureters. (A) Pie chart summarizing the results from the microarray analysis of E14.5 control and *Gata6cKO* ureters. (B,C) List of 57 genes with increased expression (FC≥2.0) (B) and list of 61 genes with decreased expression (FC≤-2.0) (C) in the microarray analysis of E14.5 *Gata6cKO* ureters. (D,E) RNA *in situ* hybridization analysis on sections of the proximal ureter at E14.5 for genes encoding components and targets of RA signaling (D) and for microarray candidates (E). (F) RT-qPCR results of expression of selected genes in three independent total RNA pools of E14.5 control and *Gata6cKO* ureters. Differences were considered non-significant (ns) at $P>0.05$ and highly significant at $^{**}P\leq0.01$; two-tailed Student's *t*-test. For values and statistics, see Table S11. (G) RNA *in situ* hybridization analysis of *Myocd* expression on sections of the proximal ureter at E15.5, E16.5 and E18.5, and of ureters explanted at E18.5 and cultured for 6 days. k, kidney; ue, ureteric epithelium; um, ureteric mesenchyme.

Given the cooperativity of GATA6 and FOXF1 in *Myocd* activation in this cellular system, we wondered whether forced expression of FOXF1 would rescue the peristaltic defects of *Gata6*-deficient ureters. For this, we combined an inducible cre driver line (*Axin2*^{creERT2}) with the floxed allele of *Gata6* (*Gata6*^{fl}) and a *Foxf1* misexpression allele (*Hprt*^{Foxf1}) (Bohnenpoll et al., 2017c), and monitored the peristaltic activity of E12.5 ureter explants after administration of 4-hydroxytamoxifen *in vitro*. *Axin2*$^{creERT2/+}$;*Gata6*$^{fl/fl}$ ureters showed a delayed onset of peristaltic activity and reduced contraction frequency compared with the control. Misexpression of *Foxf1* led to premature activation of peristaltic activity irrespective whether *Gata6* was present (in *Axin2*$^{creERT2/+}$;*Gata6*$^{fl/+}$;*Hprt*$^{Foxf1/y}$ ureters) or lost (in *Axin2*$^{creERT2/+}$;*Gata6*$^{fl/fl}$;*Hprt*$^{Foxf1/y}$ ureters) (Fig. 7B, Table S14). We conclude that FOXF1 and GATA6 both impinge on *Myocd* activation but that enhanced FOXF1 activity can override the loss of *Gata6* (Fig. 7C).

DISCUSSION

Here, we have identified GATA6 as a novel regulator of visceral SMC differentiation in the ureter. GATA6 acts downstream of

Development (2022) 149, dev200522. doi:10.1242/dev.200522

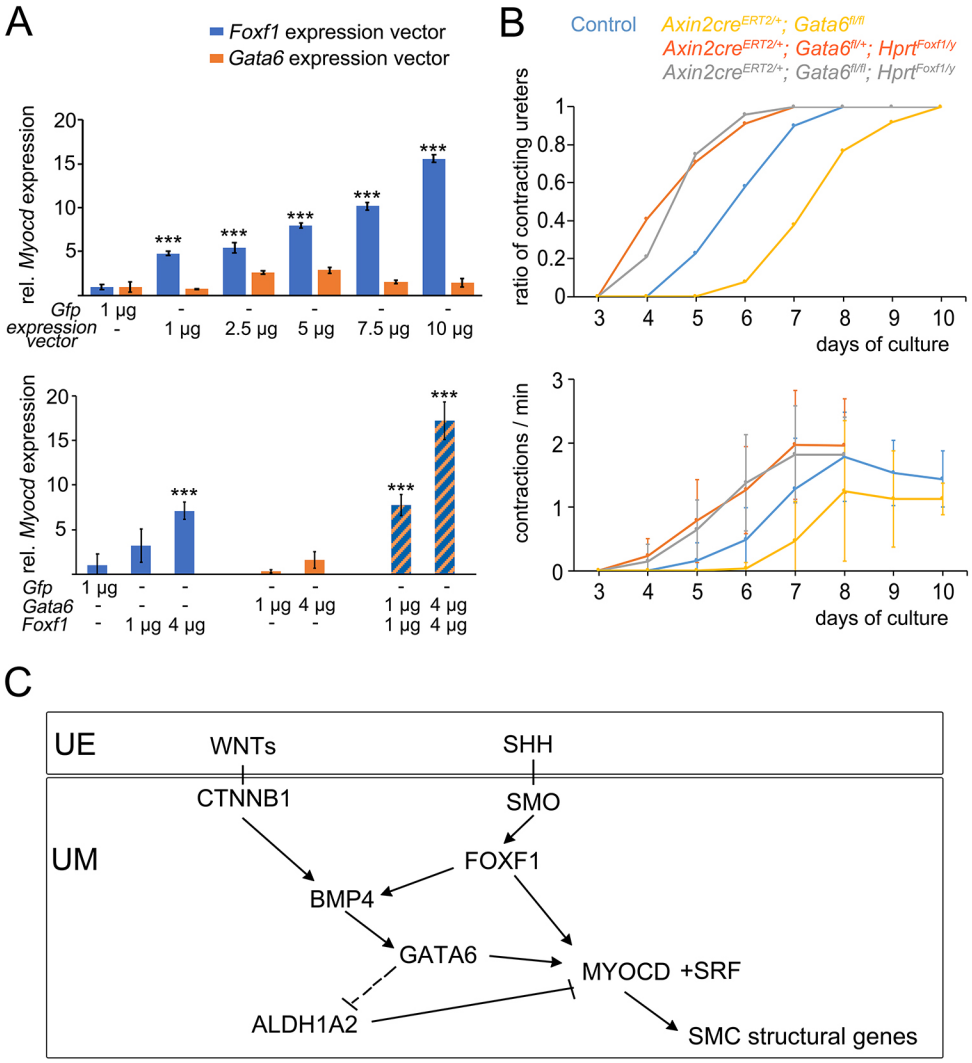

Fig. 7. GATA6 and FOXF1 cooperate in *Myocd* activation in NIH3T3 cells and in the UM *in vivo*. (A) Expression constructs for GATA6 and FOXF1 were individually (upper graph) and combinatorially (lower graph) transfected into NIH3T3 cells and the relative *Myocd* expression was determined after 2 days. For source data and statistics, see Table S13. ***$P \leq 0.0005$, two-tailed Student's *t*-test. (B) E12.5 ureters were explanted and grown for 10 days in culture. The peristaltic activity was monitored every day using video microscopy. The upper graph shows the ratio of ureters that had started peristaltic activity: control (*n*=129), *Axin2*$^{creERT2/+}$;*Gata6*$^{fl/fl}$ (*n*=13), *Axin2*$^{creERT2/+}$;*Gata6*$^{fl/+}$;*Hprt*$^{Foxf1/y}$ (*n*=34) and *Axin2*$^{creERT2/+}$;*Gata6*$^{fl/fl}$;*Hprt*$^{Foxf1/y}$ (*n*=28) ureters; the lower graph shows the contractions per min of control (*n*=71), *Axin2*$^{creERT2/+}$;*Gata6*$^{fl/fl}$ (*n*=7), *Axin2*$^{creERT2/+}$;*Gata6*$^{fl/+}$;*Hprt*$^{Foxf1/y}$ (*n*=17) and *Axin2*$^{creERT2/+}$;*Gata6*$^{fl/fl}$;*Hprt*$^{Foxf1/y}$ (*n*=14) ureters. Data are mean±sd. For source data and statistics, see Table S14. (C) Scheme showing the integration of GATA6 function in the regulatory circuit controlling *Myocd* activation and SMC differentiation in the murine ureter. SHH signals from the ureteric epithelium (UE) activate via SMO the expression of FOXF1 in the ureteric mesenchyme (UM). FOXF1 activates BMP4. BMP4 receives an additional input from epithelial WNT signals via mesenchymal CTNNB1. BMP4 induces GATA6, which possibly acts as a pioneer factor to open the *Myocd* locus. FOXF1 may act as a lineage-determining factor to activate *Myocd*, which in turn, in combination with SRF, activates SMC structural genes. *Myocd* expression/SMC differentiation is negatively affected by RA in the UM. GATA6 has a weak repression effect (indicated by stitched lines) on the expression of *Aldh1a2*, which encodes a biosynthetic enzyme for RA synthesis. Increased RA does not contribute to the delayed onset of *Myocd* expression in *Gata6cKO* UM.

BMP4 and cooperates with FOXF1 in *Myocd* activation and, thus, SMC differentiation, possibly as pioneer (GATA6) and lineage-determining factor (FOXF1) (Fig. 7C). Our work confirms that a delayed and reduced onset of SMC differentiation results in ureter dilatation at birth, and that relief from the resulting hydrostatic pressure may aid in regaining ureter peristalsis.

Gata6 is a novel regulator of visceral SMC differentiation

Previous work described expression of *Gata6* in various progenitor populations during murine development, including the visceral endoderm, the (pre-)cardiac mesoderm, and the neural crest and the endoderm of the primitive gut tube (including the bronchial tree), and also in mature SMCs of the aorta, large arteries and the bladder. These studies also reported *Gata6* expression in the urogenital ridge at E13.5 but did not further analyze expression during urinary tract development (Freyer et al., 2015; Morrisey et al., 1996; Nemer and Nemer, 2003). Our work characterizes the undifferentiated UM as an additional expression domain of *Gata6*/GATA6 in mouse development. We found downregulation of *Gata6*/GATA6 expression with onset of mesenchymal cyto-differentiation in the ureter, which contrasts with the pattern in the adjacent bladder primordium, where *Gata6* expression is maintained into adult stages (Freyer et al., 2015; Morrisey et al., 1996).

Development (2022) 149, dev200522. doi:10.1242/dev.200522

The conditional loss of *Gata6* in the UM did not affect survival, proliferation and patterning of these progenitors but led to a failure to timely activate the SMC program in the fetal ureter. This finding is in line with previous reports that *Gata6* is crucial for early differentiation of progenitors of various endodermal, mesodermal and ectodermal sources (Morrisey et al., 1998; Tevosian et al., 2015; Zhao et al., 2008, 2005) (for a review see (Tremblay et al., 2018)).

Our study stresses the significance of *Gata6* and its related family members (*Gata4* and *Gata5*) as regulators of muscle cell differentiation. Although the role of *Gata6* (in combination with *Gata4*) in early differentiation of cardiomyocytes has been appreciated for long (Zhao et al., 2008), the role in vascular, and especially in visceral, SMC differentiation has remained less clear. Some *in vitro* studies initially suggested that GATA6 induces and maintains the contractile phenotype of vascular SMCs (Abe et al., 2003; Mano et al., 1999; Wada et al., 2002), whereas others questioned such a role (Lepore et al., 2005; Yin and Herring, 2005). However, recent *in vivo* loss- and gain-of-function studies provided strong evidence that *Gata6* is both required and sufficient for the differentiation of cardiac neural crest cells into SMCs that surround the large vessels of the cardiac outflow tract (Losa et al., 2017).

Knockdown of endogenous *GATA6* in primary human bladder SMCs led to decreased mRNA levels of some SMC structural genes, suggesting a role in maintaining the differentiated phenotype of these visceral SMCs (Kanematsu et al., 2007). However, to our knowledge, an *in vivo* requirement for *Gata6* in the establishment or maintenance of the SMC phenotype in the bladder has not been reported.

It is important to note that *Gata6* expression has not been observed during visceral SMC development of the respiratory system, the urethra and the gastrointestinal tract (Morrisey et al., 1996). Moreover, a role of *Gata6* has not been reported for vascular SMCs that do not derive from neural crest cells, such as epicardium-derived coronary SMCs. We cannot exclude the possibility that low levels of expression of *Gata6* or of other Gata family members have escaped detection and/or that redundancy of several Gata genes has precluded functional insights. However, it is also conceivable that *Gata6* acts only in some of the SMC differentiation programs during embryonic development. This is in line with the finding that both vascular and visceral SMCs arise from a multitude of progenitors, and that diverse signals from adjacent epithelial and endothelial primordia (and also from within the SMC progenitors) are implicated in activation of the SMC differentiation program (Donadon and Santoro, 2021; Mack, 2011).

Our *in vivo* and *ex vivo* experiments have shown that BMP4 signaling is both required and sufficient for *Gata6* expression in the UM. Given the findings that *Gata4* and *Gata6* are co-expressed in many mesodermal and endodermal progenitors, that BMP4 is upstream of *Gata4* in the precardiac mesoderm (Schultheiss et al., 1997), endoderm (Rossi et al., 2001) and lateral plate mesoderm (Rojas et al., 2005), and that neural crest cell induction requires BMP4 signaling (Baker and Bronner-Fraser, 1997), it is tempting to speculate that BMP4 signaling-regulated expression of *Gata6* (and/or *Gata4*) defines a crucial axis in the differentiation of both cardiomyocytes and a subset of vascular and visceral SMCs.

Gata6 is required for activation of *Myocd* expression in the UM

Our molecular characterization of *Gata6cKO* ureters revealed a dramatic reduction of *Myocd* expression in the fetal ureter. MYOCD acts a transcriptional co-activator that complexes with the DNA-binding protein serum response factor (SRF) in the activation of genes that harbor binding sites for SRF, so called CArG boxes in their promoters (Norman et al., 1988; Sun et al., 2006; Wang et al., 2001; Wang and Olson, 2004). Given the fact that *Myocd* is required for SMC differentiation, downregulation of *Myocd* expression is the likely cause for SMC differentiation and peristalsis defects in *Gata6cKO* ureters.

As *Myocd* is sufficient to induce SMC differentiation when ectopically expressed (van Tuyn et al., 2005; Wang et al., 2003), temporal and spatial control of *Myocd* expression underlies the regionalized programs of visceral and vascular SMC differentiation. As mentioned above, activation of *Myocd* and, hence, of the SMC program occurs in response to a multitude of signals that are released from endothelial and epithelial primordia, as well as in response to signals secreted from the SMC progenitors (Donadon and Santoro, 2021; Mack, 2011). In the murine ureter, SHH and WNTs have been characterized as epithelial signals from the ureteric bud that maintain UM proliferation and induce *Myocd* expression and SMC differentiation. SMO-dependent SHH signaling and CTNNB1-dependent WNT signaling induce and maintain, respectively, BMP4 expression in the UM. In turn, BMP4 is required for UM proliferation, *Myocd* expression and SMC differentiation (Bohnenpoll et al., 2017c; Mamo et al., 2017; Trowe et al., 2012). Importantly, we neither detected changes in expression of the ligand genes *Shh*, *Wnt* and *Bmp4* nor alterations in their signaling activities in the UM of *Gata6cKO* ureters. Furthermore, we found unaltered expression of transcription factors, including *Foxf1*, that impinge on *Myocd* expression downstream of the activity of these signaling pathways in the UM. These data show that all known positive molecular inputs on *Myocd* expression in the UM are unaffected by loss of *Gata6*. This is notable as several studies suggested that *Gata6* acts as a regulator of *Bmp4* expression in some developmental settings (Nemer and Nemer, 2003; Peterkin et al., 2003; Whissell et al., 2014; Zeng and Childs, 2012).

Our *Gata6cKO* analysis detected increased expression of RA synthesizing enzymes in the early ureter, and slightly increased expression of some RA-dependent genes in the UM. Pharmacological inhibition of RA signaling did not alleviate the SMC defects but increased them, making it unlikely that RA, which is known to inhibit SMC differentiation in the UM (Bohnenpoll et al., 2017b), causes or contributes to the lack of *Myocd* activation in *Gata6cKO* UM. Increased RA signaling may, however, contribute to the slight delay in epithelial stratification and differentiation, and/or occurrence of a neuronal expression profile in the mutant ureter, as suggested by some studies (Bohnenpoll et al., 2017b; Lakard et al., 2007; Sidell and Horn, 1985).

Based on these results, we posit that GATA6 presents a novel and direct input on *Myocd* activation in the UM. This assumption receives indirect but strong support from a recent report that *Gata6* is required for *Myocd e*xpression in cardiac neural crest cells, and that it occupies a binding site in the *Myocd* locus (Losa et al., 2017).

It is important to note that GATA6 expression occurs in the undifferentiated UM from E11.5 to E14.5, i.e. much earlier than that of *Myocd*, which can be detected from E14.5 onwards. Moreover, GATA6 was not sufficient to induce *Myocd* expression in NIH3T3 cells but enhanced the activity of FOXF1 in doing so. This parallels our earlier finding that BMP4 signaling, i.e. the activator of *Gata6* expression, is not sufficient to activate the SMC program in the ureter but synergizes with FOXF1 (Bohnenpoll et al., 2017c). Given recent reports on the molecular function of GATA6 as a chromatin remodeling protein and pioneer factor in cardiac and endoderm development (Heslop et al., 2021; Sharma et al., 2020), and the occurrence of a binding site in the *Myocd* locus in neural crest cells

Development (2022) 149, dev200522. doi:10.1242/dev.200522

(Losa et al., 2017), we hypothesize that GATA6 opens chromatin in and around the *Myocd* locus in the UM to ease subsequent binding of FOXF1 and to ensure precise temporal activation of *Myocd* transcription.

FOXF1 was not only sufficient to induce *Myocd* expression in NIH3T3 cells, it also led to premature activation of the SMC program upon forced overexpression in the UM. As the latter activity was independent of *Gata6,* it shows that FOXF1 acts as the dominant lineage-determining factor. Occurrence of *Myocd* expression and SMC differentiation in *Gata6cKO* ureters at E18.5 and at later stages in *ex vivo* cultures, may indicate that FOXF1 expression had sufficiently increased to open the *Myocd* locus and activate its transcription.

Interestingly, with the exception of *Tnnt2*, all of the SMC structural genes evaluated returned to normal expression levels in extended *ex vivo* cultures of *Gata6cKO* explants. As GATA6 binds and transactivates a cardiac-specific enhancer element in the *Tnnc1* gene (Morrisey et al., 1996), it is conceivable that *Tnnt2* presents an additional direct target of GATA6 activity in the UM.

Gata2 and *Gata6* genes regulate distinct subprograms of ureteric SMC differentiation

We have recently reported that *Gata2* is expressed in the UM and that its conditional loss leads to a delayed onset of SMC differentiation, ureter dilatation in fetal life and hydroureternephrosis after birth (Weiss et al., 2019). Given the co-expression of *Gata6* with *Gata2* in the UM, and the strong similarity of phenotypic changes of the upper urinary tract upon individual loss in the UM, it appeared possible that *Gata2* and *Gata6* act in a common pathway for *Myocd* activation. However, our analyses showed that the two genes are differentially regulated (*Gata6* depends on BMP4, *Gata2* on RA signaling), and that the loss of the genes in the UM leads to different molecular changes at E14.5. Although GATA2, at least partially, acts as a feed-back inhibitor for RA signaling (Weiss et al., 2019), deregulation of RA signaling is irrelevant for the SMC defects in *Gata6cKO* ureters, and direct regulation of *Myocd* seems likely. Moreover, we did not find genetic interaction when combining loss-of-function alleles of both genes. Last but not least, GATA2 and GATA6 belong to different subfamilies, the members of which preferentially interact with themselves (Tremblay et al., 2018).

Similar to *Gata2*-deficient ureters, *Gata6cKO* ureters had a normal excitation and/or conduction machinery, and regained considerable peristaltic performance when relieved from urinary pressure in an *ex vivo* culture setting. Although this confirms that increased hydrostatic pressure exacerbates the SMC defects *in vivo*, it highlights that a temporary artificial bypass *in vivo* may provide an opportunity for the mesenchymal coat to (re-)differentiate contractile SMCs and regain peristaltic activity. Irrespective of future therapeutic options for congenital forms of hydroureter formation in humans, *Gata6* and *Gata2* are candidates to include in mutational screens for monogenetic causes of this disease entity.

MATERIALS AND METHODS

Mouse work

Mice with conditional inactivation of *Gata6* (*Gata6*$^{tm2.1Sad}$, synonym *Gata6*$^{fl/fl}$) (Sodhi et al., 2006) were obtained from Joerg Heineke (previously Medizinische Hochschule Hannover, now Medical Faculty Mannheim, Germany) after permission from Steve Duncan (Medical University of South Carolina, Charleston, USA); mice with conditional inactivation of *Bmp4* (*Bmp4*^{tm3Blh}, synonym *Bmp4*^{fl}) (Kulessa and Hogan, 2002) were a gift from Rolf Zeller (University of Basel, Switzerland) after permission from Brigid Hogan (Duke University Medical Center, Durham, NC, USA). Rolf Kemler (Max-Planck-Institute for Immunobiology and Epigenetics, Freiburg, Germany) provided mice with conditional inactivation of β-catenin (*Ctnnb1*) (*Ctnnb1*^{tm2Kem}, synonym *Ctnnb1*^{fl}) (Brault et al., 2001). Mice with conditional inactivation of smoothened (*Smo*) (*Smo*^{tm2Amc}, synonyms *Smo*^{fl} and JAX 004526) (Long et al., 2001) were purchased from the Jackson Laboratory, as were mice with a *creERT2* knock-in allele of *Axin2* [*Axin2*$^{tm1(cre/ERT2)Rnu}$, synonyms *Axin2*^{creERT2} and JAX #018867] (van Amerongen et al., 2012). The *cre* driver line *Tbx18*$^{tm4(cre)Akis}$ (synonym *Tbx18*^{cre}) and the *Foxf1* misexpression allele [*Hprt*$^{tm1(CAG-Foxf1,-EGFP)Akis}$, synonym: *Hprt*^{Foxf1}] were previously generated in house (Airik et al., 2010; Bohnenpoll et al., 2017c).

All mouse lines were maintained on an NMRI outbred background. NMRI wild-type embryos were used for expression analysis. Embryos for phenotypic analyses were derived from matings of males double heterozygous for *Tbx18*^{cre} line and the floxed loss-of-function allele with females homozygous for the same floxed loss-of-function allele. Littermates without the *Tbx18*^{cre} allele were used as controls. For timed pregnancies, vaginal plugs were checked on the morning after mating; noon was designated to be E0.5. Embryos and urogenital systems were dissected in PBS. Specimens were fixed in 4% PFA/PBS, transferred to methanol and stored at −20°C prior to further processing. PCR genotyping was performed on genomic DNA prepared from yolk sacs or liver biopsies. The experiments were approved by the local Institutional Animal Care and Research Advisory Committee and permitted by the Lower Saxony State Office for Consumer Protection and Food Safety (reference number 42500/1H).

Organ cultures

Ureters (experiments in Figs 5 and 7, Fig. S13) and ureters with kidneys (experiment in Fig. S8) were dissected from the embryo, explanted on 0.4 µm polyester membrane Transwell supports (3450, Corning) and cultured at the air-liquid interface with DMEM/F12 supplemented with 1% of concentrated stocks of penicillin/streptomycin, sodium pyruvate, glutamax and non-essential amino acids (21331020, 15140122, 11360070, 35050038 and 11140035, Thermo Fisher Scientific) with 10% FCS (S0115, Biochrom) (experiments in Fig. 5) or without FCS (experiment Fig. S8), or with IST-G (insulin-transferrin-selenium, 41400045, Thermo Fisher Scientific) (experiments in Fig. 7). To induce recombination with the *Axin2*^{creERT2} line, 4-hydroxytamoxifen (H7904, Sigma-Aldrich) was used at a final concentration of 500 nM. Recombinant mouse BMP4 (5020-BP, R&D Systems) was dissolved in 4 mM HCl to a final concentration of 100 ng/ml. The BMP4 inhibitor noggin (ZO3205, Biozol/GenScript) was dissolved in water to 10 µg/ml. BMS493 (3509, Tocris BioScience) or RA (0695, Tocris BioScience) was dissolved in DMSO and added to the medium at a final concentration of 1 µM. The culture medium was replaced every second day. Contralateral kidneys were used as controls. For video documentation, the cultures were acclimatized to room conditions and then imaged in a bright-field channel for 1 min at a rate of 5 frames per second. Measurement of the contractions per minute and the peristaltic intensity was carried out either manually or via computational Fiji Multi-Kymograph analysis (Schindelin et al., 2012). Therefore, the length of the ureter was subdivided into 25 (proximal level), 50 (medial level) or 75 (distal level) percentiles. One contraction was set to 100 frames representing 20 s in real time. Kymograph grey values were divided by the maximum grey value and ratios were plotted with Microsoft Excel.

Histological analysis

Embryos and urogenital systems were embedded in paraffin and sectioned at 5 µm. Hematoxylin and Eosin staining was performed according to standard procedures. Ink injection experiments were performed as described previously (Airik et al., 2006).

RNA *in situ* hybridization analysis

Section *in situ* hybridization on 10 µm paraffin wax-embedded sections was performed as previously described (Moorman et al., 2001). Whole mount *in situ* hybridization of whole-kidney rudiments or kidney cultures followed

Development (2022) 149, dev200522. doi:10.1242/dev.200522

a standard procedure with digoxigenin-labeled antisense riboprobes (Wilkinson and Nieto, 1993).

Reverse transcription-quantitative polymerase chain reaction

Total RNA was isolated from three pools of 10 ureters each of E14.5 control and *Gata6cKO* embryos using TRIzol (15596-018, Thermo Fisher Scientific). cDNA was synthesized from 2.5 µg total RNA applying RevertAid H Minus reverse transcriptase (EP0452, Thermo Fisher Scientific) as described previously (Thiesler et al., 2021). The NCBI tool Primer3 version4.1 was used to design specific primers (Table S15). Reverse transcription-quantitative polymerase chain reaction (RT-qPCR) was performed in 10 µl 1:2 diluted BIO SyGreen Lo-ROX mix (PCR Biosystems) with 400 nM primers and 1 ng/µl cDNA applying a QuantStudio3 PCR system fluorometric thermal cycler (Thermo Fisher Scientific). Each of the three biological replicates represents the average of four technical replicates. Data were processed by QuantStudio data analysis software (version1.5.1, Thermo Fisher Scientific) using the comparative threshold cycle ($\Delta\Delta C_T$) method with *Gapdh* (Werneburg et al., 2015) and *Ppia* as reference genes.

Microarray analysis

Two pools of 10 E14.5 ureters, from male and female control embryos and from *Gata6cKO* embryos, were collected. Total RNA was extracted using peqGOLD RNApure (product 732-3312, order 30-1010, PeqLab Biotechnologie) and subsequently sent to the Research Core Unit Transcriptomics of Hannover Medical School where RNA was Cy3 labeled and hybridized to Agilent Whole Mouse Genome Oligo v2 (4×44 K) microarrays (G4846A, Agilent Technologies). To identify differentially expressed genes, normalized expression data were filtered using Excel based on an intensity threshold of 100 and a more than 1.9-fold change in all pools**.** Microarray data have been deposited in GEO under accession number GSE174614.

Immunofluorescent detection of antigens

For immunofluorescent staining, 5 µm paraffin wax-embedded sections were stained as previously described (Bohnenpoll et al., 2017a). Primary antibodies and dilutions were as follows: goat-anti-GATA6 (1:50, AF1700, R&D Systems), rabbit-anti-GATA6 (1:200, 5851, Cell Signaling Technology), mouse-anti-ACTA2 (1:500, A5228, Sigma-Aldrich), rabbit-anti-TAGLN (1:200, ab14106, Abcam), rabbit-anti-ΔNP63 (1:250, 619001, BioLegend), rabbit-anti-KRT5 (1:250, PRB-160P, BioLegend), mouse-anti-UPK1B (1:200, WH0007348 M, Sigma-Aldrich), rabbit-anti-TBX2 (1:200, 07-318, Merck Millipore), goat-anti-TBX3 (1:500, sc-31656, Santa Cruz Biotechnology), rabbit-anti-HCN3 (1:200, ab5506, Abcam) and rabbit-anti-KIT (1:200, ab5506, Abcam). (The last two antibodies are no longer available.) Secondary antibodies and dilutions were as follows: goat-anti-rabbit Alexa488 (1:250, A11034, Invitrogen), donkey-anti-mouse Alexa488 (1:250, A21202, Invitrogen), goat-anti-mouse Alexa555 (1:500, A21422, Invitrogen), biotinylated goat-anti-rabbit (1:200, 111065033, Dianova) and biotinylated donkey-anti-goat (1:200, 705-065-003, Dianova), Biotin-SP-conjugated Fab fragment goat anti-rabbit IgG (H+L) (1:400, 111-067-003, Jackson ImmunoResearch Labs, ordered via Dianova) and streptavidin HRP (1:500, 434323, Thermo Fisher Scientific). For amplification of the antibodies, the TSA Tetramethylrhodamine Amplification Kit (1:100, NEL701001KT, PerkinElmer) was used. After antigen retrieval (H-3300, Antigen Unmasking Solution, Vector Laboratories; 15 min, 100°C), labeling of primary antibodies was performed overnight at 4°C. Labeling of secondary antibodies was performed for 1 h at room temperature in blocking solution.

Cell proliferation and apoptosis assays

Cell proliferation rates were investigated by the detection of incorporated BrdU on 5 µm paraffin sections according to published protocols (Bussen et al., 2004). For the analysis, 12 sections per specimen (n=3) and genotype of the proximal ureter were stained. The BrdU-labeling index was defined as the number of BrdU-positive nuclei relative to the total number of nuclei, as detected by counterstaining of nuclei with 4′,6-diamidino-2-phenylindole (DAPI, 6335.1, Carl Roth) in histologically defined compartments of the ureter. Apoptosis in tissues was assessed by the TUNEL assay using the ApopTag Plus Fluorescein *In Situ* Apoptosis Detection Kit (S7111, Merck) on 5 µm paraffin wax-embedded sections.

Transfection experiments and *Myocd* expression analysis in NIH3T3 cells

The *Gata6* open reading frame was amplified from a *pCI* vector (a kind gift from Joerg Heineke) and subcloned as a NcoI-NdeI fragment into a *pSP64 in vitro* transcription vector containing globin leader and trailer sequences and a MYC or HA tag, respectively (Farin et al., 2007). Tagged *Gata6* was then shuttled as a HindIII-EcoRI fragment into *pcDNA3* for eukaryotic expression. *Foxf1 pCMV6*-entry expression vector was obtained from Origene (MR225056).

NIH3T3 cells were seeded on six-well plates and grown to 70-80% confluency. For each experiment, three independent six-well plates were transfected with increasing amount of plasmids with Lipofectamine 2000 Transfection Reagent (11668027, ThermoFisher) following the manufacturer's recommendations. After 2 days, cells were harvested, total RNA was extracted with peqGOLD RNApure (30-1020, PeqLab) and first-strand cDNA synthesis was performed with RevertAid reverse transcriptase (EP0441, ThermoFisher). To quantify *Myocd* expression in NIH3T3 cells, a semi-quantitative PCR was established with *Myocd*-specific primers (forward, TGAGACTCACCATGACACTCC; reverse, TGGCGGTATTAAGCCTTGGT), and adjustment of the number of cycles to the mid-logarithmic phase. Annealing was performed at 56°C for 20 s, extension at 72°C for 20 s with 25-30 cycles. Quantification was performed with ImageJ (Schneider et al., 2012). *Gapdh* was used for normalization (Tanimizu and Miyajima, 2004).

Statistics

For statistical analysis, the two-tailed Student's *t*-test was performed and the data were expressed as mean±s.d. For relative analyses, wild-type values were set to 1. Differences were considered significant at $*P<0.05$, highly significant at $**P\leq0.005$ and extremely significant at $***P\leq 0.0005$.

Image documentation

Sections and organ cultures were photographed using a DM5000 microscope (Leica Camera) with Leica DFC300FX digital camera or a Leica DM6000 microscope with Leica DFC350FX digital camera. Urogenital systems were documented using a Leica M420 microscope with a Fujix HC-300Z digital camera (Fujifilm Holdings). Whole-mount *in situ* hybridization of cultured kidney rudiments were documented using a Leica Z6 APO microscope with a Leica DFC420C digital camera. Figures were prepared with Adobe Photoshop CS3 and CS4.

Acknowledgements

We thank Rolf Kemler, Rolf Zeller and Brigid Hogan for mice; Swagata Goswami, Patricia Zarnovican and Imke Peters for help; Rita Gerardy-Schahn for lab space; and the Research Core Unit Transcriptomics of Hannover Medical School for microarray analysis. Some data of this study form part of a PhD thesis (J.K., Gottfried Wilhelm Leibniz Universität Hannover, 2021).

Competing interests

The authors declare no competing or financial interests.

Author contributions

Conceptualization: J.K., A.K.; Methodology: J.K., T.H.-W.L., M.-O.T., H.T.; Formal analysis: J.K., A.-C.W., T.H.-W.L., L.D., M.-O.T., H.T.; Investigation: J.K., A.-C.W., T.H.-W.L., L.D., M.-O.T., H.T.; Resources: J.H., S.A.D., A.K.; Data curation: J.K., A.-C.W., T.H.-W.L., L.D., M.-O.T., H.T.; Writing - original draft: J.K., A.K.; Writing - review & editing: J.K., A.-C.W., T.H.-W.L., L.D., M.-O.T., H.T., H.H., J.H., S.A.D., A.K.; Visualization: T.H.-W.L., L.D.; Supervision: A.-C.W., H.H., A.K.; Project administration: A.K.; Funding acquisition: A.K.

Funding

This work was supported by grants from by the Deutsche Forschungsgemeinschaft (German Research Foundation) (DFG KI 728/7-2 and DFG KI728/9-2 to A.K.).

Data availability

Microarray data have been deposited in GEO under accession number GSE174614.

References

Abe, M., Hasegawa, K., Wada, H., Morimoto, T., Yanazume, T., Kawamura, T., Hirai, M., Furukawa, Y. and Kita, T. (2003). GATA-6 is involved in PPARγ-mediated activation of differentiated phenotype in human vascular smooth muscle cells. *Arterioscler. Thromb. Vasc. Biol.* **23**, 404-410. doi:10.1161/01.ATV.0000059405.51042.A0

Airik, R., Bussen, M., Singh, M. K., Petry, M. and Kispert, A. (2006). Tbx18 regulates the development of the ureteral mesenchyme. *J. Clin. Invest.* **116**, 663-674. doi:10.1172/JCI26027

Airik, R., Trowe, M.-O., Foik, A., Farin, H. F., Petry, M., Schuster-Gossler, K., Schweizer, M., Scherer, G., Kist, R. and Kispert, A. (2010). Hydroureteronephrosis due to loss of Sox9-regulated smooth muscle cell differentiation of the ureteric mesenchyme. *Hum. Mol. Genet.* **19**, 4918-4929. doi:10.1093/hmg/ddq426

Aydogdu, N., Rudat, C., Trowe, M. O., Kaiser, M., Lüdtke, T. H., Taketo, M. M., Christoffels, V. M., Moon, A. and Kispert, A. (2018). TBX2 and TBX3 act downstream of canonical WNT signaling in patterning and differentiation of the mouse ureteric mesenchyme. *Development* **145**, dev171827. doi:10.1242/dev.171827

Baker, C. V. and Bronner-Fraser, M. (1997). The origins of the neural crest. Part I: embryonic induction. *Mech. Dev.* **69**, 3-11. doi:10.1016/S0925-4773(97)00132-9

Bohnenpoll, T. and Kispert, A. (2014). Ureter growth and differentiation. *Semin. Cell Dev. Biol.* **36**, 21-30. doi:10.1016/j.semcdb.2014.07.014

Bohnenpoll, T., Bettenhausen, E., Weiss, A.-C., Foik, A. B., Trowe, M.-O., Blank, P., Airik, R. and Kispert, A. (2013). Tbx18 expression demarcates multipotent precursor populations in the developing urogenital system but is exclusively required within the ureteric mesenchymal lineage to suppress a renal stromal fate. *Dev. Biol.* **380**, 25-36. doi:10.1016/j.ydbio.2013.04.036

Bohnenpoll, T., Feraric, S., Nattkemper, M., Weiss, A.-C., Rudat, C., Meuser, M., Trowe, M.-O. and Kispert, A. (2017a). Diversification of cell lineages in ureter development. *J. Am. Soc. Nephrol.* **28**, 1792-1801. doi:10.1681/ASN.2016080849

Bohnenpoll, T., Weiss, A.-C., Labuhn, M., Lüdtke, T. H., Trowe, M.-O. and Kispert, A. (2017b). Retinoic acid signaling maintains epithelial and mesenchymal progenitors in the developing mouse ureter. *Sci. Rep.* **7**, 14803. doi:10.1038/s41598-017-14790-2

Bohnenpoll, T., Wittern, A. B., Mamo, T. M., Weiss, A.-C., Rudat, C., Kleppa, M.-J., Schuster-Gossler, K., Wojahn, I., Lüdtke, T. H., Trowe, M.-O. et al. (2017c). A SHH-FOXF1-BMP4 signaling axis regulating growth and differentiation of epithelial and mesenchymal tissues in ureter development. *PLoS Genet.* **13**, e1006951. doi:10.1371/journal.pgen.1006951

Brault, V., Moore, R., Kutsch, S., Ishibashi, M., Rowitch, D. H., McMahon, A. P., Sommer, L., Boussadia, O. and Kemler, R. (2001). Inactivation of the β-catenin gene by Wnt1-Cre-mediated deletion results in dramatic brain malformation and failure of craniofacial development. *Development* **128**, 1253-1264. doi:10.1242/dev.128.8.1253

Bussen, M., Petry, M., Schuster-Gossler, K., Leitges, M., Gossler, A. and Kispert, A. (2004). The T-box transcription factor Tbx18 maintains the separation of anterior and posterior somite compartments. *Genes Dev.* **18**, 1209-1221. doi:10.1101/gad.300104

Caubit, X., Lye, C. M., Martin, E., Coré, N., Long, D. A., Vola, C., Jenkins, D., Garratt, A. N., Skaer, H., Woolf, A. S. et al. (2008). Teashirt 3 is necessary for ureteral smooth muscle differentiation downstream of SHH and BMP4. *Development* **135**, 3301-3310. doi:10.1242/dev.022442

Chazaud, C., Dollé, P., Rossant, J. and Mollard, R. (2003). Retinoic acid signaling regulates murine bronchial tubule formation. *Mech. Dev.* **120**, 691-700. doi:10.1016/S0925-4773(03)00048-0

Chiodini, B., Ghassemi, M., Khelif, K. and Ismaili, K. (2019). Clinical outcome of children with antenatally diagnosed hydronephrosis. *Front. Pediatr.* **7**, 103. doi:10.3389/fped.2019.00103

David, S. G., Cebrian, C., Vaughan, E. D., Jr. and Herzlinger, D. (2005). c-kit and ureteral peristalsis. *J. Urol.* **173**, 292-295. doi:10.1097/01.ju.0000141594.99139.3d

Donadon, M. and Santoro, M. M. (2021). The origin and mechanisms of smooth muscle cell development in vertebrates. *Development* **148**, dev197384. doi:10.1242/dev.197384

Dudley, J. A., Haworth, J. M., McGraw, M. E., Frank, J. D. and Tizard, E. J. (1997). Clinical relevance and implications of antenatal hydronephrosis. *Arch. Dis. Child. Fetal Neonatal. Ed.* **76**, F31-F34. doi:10.1136/fn.76.1.F31

Ek, S., Lidefeldt, K. J. and Varricio, L. (2007). Fetal hydronephrosis; Prevalence, natural history and postnatal consequences in an unselected population. *Acta Obstet. Gynecol. Scand.* **86**, 1463-1466. doi:10.1080/00016340701714802

Farin, H. F., Bussen, M., Schmidt, M. K., Singh, M. K., Schuster-Gossler, K. and Kispert, A. (2007). Transcriptional repression by the T-box proteins Tbx18 and Tbx15 depends on Groucho corepressors. *J. Biol. Chem.* **282**, 25748-25759. doi:10.1074/jbc.M703724200

Freyer, L., Schröter, C., Saiz, N., Schrode, N., Nowotschin, S., Martinez-Arias, A. and Hadjantonakis, A. K. (2015). A loss-of-function and H2B-Venus transcriptional reporter allele for Gata6 in mice. *BMC Dev. Biol.* **15**, 38. doi:10.1186/s12861-015-0086-5

Häfner, R., Bohnenpoll, T., Rudat, C., Schultheiss, T. M. and Kispert, A. (2015). Fgfr2 is required for the expansion of the early adrenocortical primordium. *Mol. Cell. Endocrinol.* **413**, 168-177. doi:10.1016/j.mce.2015.06.022

Herthelius, M., Axelsson, R. and Lidefelt, K. J. (2020). Antenatally detected urinary tract dilatation: a 12-15-year follow-up. *Pediatr. Nephrol.* **35**, 2129-2135. doi:10.1007/s00467-020-04659-4

Heslop, J. A., Pournasr, B., Liu, J. T. and Duncan, S. A. (2021). GATA6 defines endoderm fate by controlling chromatin accessibility during differentiation of human-induced pluripotent stem cells. *Cell Rep.* **35**, 109145. doi:10.1016/j.celrep.2021.109145

Hollnagel, A., Oehlmann, V., Heymer, J., Rüther, U. and Nordheim, A. (1999). Id genes are direct targets of bone morphogenetic protein induction in embryonic stem cells. *J. Biol. Chem.* **274**, 19838-19845. doi:10.1074/jbc.274.28.19838

Huang da, W., Sherman, B. T. and Lempicki, R. A. (2009). Systematic and integrative analysis of large gene lists using DAVID bioinformatics resources. *Nat. Protoc.* **4**, 44-57. doi:10.1038/nprot.2008.211

Hurtado, R., Bub, G. and Herzlinger, D. (2010). The pelvis-kidney junction contains HCN3, a hyperpolarization-activated cation channel that triggers ureter peristalsis. *Kidney Int.* **77**, 500-508. doi:10.1038/ki.2009.483

Ingham, P. W. and McMahon, A. P. (2001). Hedgehog signaling in animal development: paradigms and principles. *Genes Dev.* **15**, 3059-3087. doi:10.1101/gad.938601

Jho, E.-H., Zhang, T., Domon, C., Joo, C.-K., Freund, J.-N. and Costantini, F. (2002). Wnt/β-catenin/Tcf signaling induces the transcription of Axin2, a negative regulator of the signaling pathway. *Mol. Cell. Biol.* **22**, 1172-1183. doi:10.1128/MCB.22.4.1172-1183.2002

Kanematsu, A., Ramachandran, A. and Adam, R. M. (2007). GATA-6 mediates human bladder smooth muscle differentiation: involvement of a novel enhancer element in regulating alpha-smooth muscle actin gene expression. *Am. J. Physiol. Cell Physiol.* **293**, C1093-C1102. doi:10.1152/ajpcell.00225.2007

Kodo, K., Nishizawa, T., Furutani, M., Arai, S., Yamamura, E., Joo, K., Takahashi, T., Matsuoka, R. and Yamagishi, H. (2009). GATA6 mutations cause human cardiac outflow tract defects by disrupting semaphorin-plexin signaling. *Proc. Natl. Acad. Sci. USA* **106**, 13933-13938. doi:10.1073/pnas.0904744106

Koutsourakis, M., Langeveld, A., Patient, R., Beddington, R. and Grosveld, F. (1999). The transcription factor GATA6 is essential for early extraembryonic development. *Development* **126**, 723-732. doi:10.1242/dev.126.4.723

Kulessa, H. and Hogan, B. L. (2002). Generation of a loxP flanked bmp4loxP-lacZ allele marked by conditional lacZ expression. *Genesis* **32**, 66-68. doi:10.1002/gene.10032

Lakard, S., Lesniewska, E., Michel, G., Lakard, B., Morrand-Villeneuve, N. and Versaux-Botteri, C. (2007). In vitro induction of differentiation by retinoic acid in an immortalized olfactory neuronal cell line. *Acta Histochem.* **109**, 111-121. doi:10.1016/j.acthis.2006.10.001

Lepore, J., Cappola, T. P., Mericko, P. A., Morrisey, E. E. and Parmacek, M. S. (2005). GATA-6 regulates genes promoting synthetic functions in vascular smooth muscle cells. *Arterioscler. Thromb. Vasc. Biol.* **25**, 309-314. doi:10.1161/01.ATV.0000152725.76020.3c

Lepore, J. J., Merick, o. P. A., Cheng, L., Lu, M. M., Morrisey, E. E. and Parmacek, M. S. (2006). GATA-6 regulates semaphorin 3C and is required in cardiac neural crest for cardiovascular morphogenesis. *J. Clin. Invest.* **116**, 929-939. doi:10.1172/JCI27363

Long, F., Zhang, X. M., Karp, S., Yang, Y. and McMahon, A. P. (2001). Genetic manipulation of hedgehog signaling in the endochondral skeleton reveals a direct role in the regulation of chondrocyte proliferation. *Development* **128**, 5099-5108. doi:10.1242/dev.128.24.5099

Losa, M., Latorre, V., Andrabi, M., Ladam, F., Sagerström, C., Novoa, A., Z, P., Bridoux, L., Hanley, N. A., Mallo, M. et al. (2017). A tissue-specific, Gata6–driven transcriptional program instructs remodeling of the mature arterial tree. *Elife* **6**, e31362. doi:10.7554/eLife.31362

Mack, C. P. (2011). Signaling mechanisms that regulate smooth muscle cell differentiation. *Arterioscler. Thromb. Vasc. Biol.* **31**, 1495-1505. doi:10.1161/ATVBAHA.110.221135

Mamo, T. M., Wittern, A. B., Kleppa, M.-J., Bohnenpoll, T., Weiss, A.-C. and Kispert, A. (2017). BMP4 uses several different effector pathways to regulate proliferation and differentiation in the epithelial and mesenchymal tissue compartments of the developing mouse ureter. *Hum. Mol. Genet.* **26**, 3553-3563. doi:10.1093/hmg/ddx242

Mano, T., Luo, Z., Malendowicz, S. L., Evans, T. and Walsh, K. (1999). Reversal of GATA-6 downregulation promotes smooth muscle differentiation and inhibits intimal hyperplasia in balloon-injured rat carotid artery. *Circ. Res.* **84**, 647-654. doi:10.1161/01.RES.84.6.647

Mendelsohn, C., Ruberte, E., LeMeur, M., Morriss-Kay, G. and Chambon, P. (1991). Developmental analysis of the retinoic acid-inducible RAR-beta 2

promoter in transgenic animals. *Development* **113**, 723-734. doi:10.1242/dev.113.3.723

Moorman, A. F. M., Houweling, A. C., de Boer, P. A. J. and Christoffels, V. M. (2001). Sensitive nonradioactive detection of mRNA in tissue sections: novel application of the whole-mount in situ hybridization protocol. *J. Histochem. Cytochem.* **49**, 1-8. doi:10.1177/002215540104900101

Morrisey, E. E., Ip, H. S., Lu, M. M. and Parmacek, M. S. (1996). GATA-6: a zinc finger transcription factor that is expressed in multiple cell lineages derived from lateral mesoderm. *Dev. Biol.* **177**, 309-322. doi:10.1006/dbio.1996.0165

Morrisey, E. E., Tang, Z., Sigrist, K., Lu, M. M., Jiang, F., Ip, H. S. and Parmacek, M. S. (1998). GATA6 regulates HNF4 and is required for differentiation of visceral endoderm in the mouse embryo. *Genes Dev.* **12**, 3579-3590. doi:10.1101/gad.12.22.3579

Nemer, G. and Nemer, M. (2003). Transcriptional activation of BMP-4 and regulation of mammalian organogenesis by GATA-4 and –6. *Dev. Biol.* **254**, 131-148. doi:10.1016/S0012-1606(02)00026-X

Norman, C., Runswick, M., Pollock, R. and Treisman, R. (1988). Isolation and properties of cDNA clones encoding SRF, a transcription factor that binds to the c-fos serum response element. *Cell* **55**, 989-1003. doi:10.1016/0092-8674(88)90244-9

Perlman, H., Suzuki, E., Simonson, M., Smith, R. C. and Walsh, K. (1998). GATA-6 induces p21(Cip1) expression and G1 cell cycle arrest. *J. Biol. Chem.* **273**, 13713-13718. doi:10.1074/jbc.273.22.13713

Peterkin, T., Gibson, A. and Patient, R. (2003). GATA-6 maintains BMP-4 and Nkx2 expression during cardiomyocyte precursor maturation. *EMBO J.* **22**, 4260-4273. doi:10.1093/emboj/cdg400

Rojas, A., De Val, S., Heidt, A. B., Xu, S. M., Bristow, J. and Black, B. L. (2005). Gata4 expression in lateral mesoderm is downstream of BMP4 and is activated directly by Forkhead and GATA transcription factors through a distal enhancer element. *Development* **132**, 3405-3417. doi:10.1242/dev.01913

Rossi, J. M., Dunn, N. R., Hogan, B. L. and Zaret, K. S. (2001). Distinct mesodermal signals, including BMPs from the septum transversum mesenchyme, are required in combination for hepatogenesis from the endoderm. *Genes Dev.* **15**, 1998-2009. doi:10.1101/gad.904601

Schindelin, J., Arganda-Carreras, I., Frise, E., Kaynig, V., Longair, M., Pietzsch, T., Preibisch, S., Rueden, C., Saalfeld, S., Schmid, B. et al. (2012). Fiji: an open-source platform for biological-image analysis. *Nat. Methods* **9**, 676-682. doi:10.1038/nmeth.2019

Schneider, C. A., Rasband, W. S. and Eliceiri, K. W. (2012). NIH Image to ImageJ: 25 years of image analysis. *Nat. Methods* **9**, 671-675. doi:10.1038/nmeth.2089

Schultheiss, T. M., Burch, J. B. and Lassar, A. B. (1997). A role for bone morphogenetic proteins in the induction of cardiac myogenesis. *Genes Dev.* **11**, 451-462. doi:10.1101/gad.11.4.451

Sharma, A., Wasson, L. K., Willcox, J. A., Morton, S. U., Gorham, J. M., DeLaughter, D. M., Neyazi, M., Schmid, M., Agarwal, R., Jang, M. Y. et al. (2020). GATA6 mutations in hiPSCs inform mechanisms for maldevelopment of the heart, pancreas, and diaphragm. *Elife* **9**, e53278. doi:10.7554/eLife.53278

Sidell, N. and Horn, R. (1985). Properties of human neuroblastoma cells following induction by retinoic acid. *Prog. Clin. Biol. Res.* **175**, 39-53.

Sodhi, C. P., Li, J. and Duncan, S. A. (2006). Generation of mice harbouring a conditional loss-of-function allele of Gata6. *BMC Dev. Biol.* **6**, 19. doi:10.1186/1471-213X-6-19

Sun, Q., Chen, G., Streb, J. W., Long, X., Yang, Y., Stoeckert, C. J., Jr. and Miano, J. M. (2006). Defining the mammalian CArGome. *Genome Res.* **16**, 197-207. doi:10.1101/gr.4108706

Tanimizu, N. and Miyajima, A. (2004). Notch signaling controls hepatoblast differentiation by altering the expression of liver-enriched transcription factors. *J. Cell Sci.* **117**, 3165-3174. doi:10.1242/jcs.01169

Tevosian, S. G., Jiménez, E., Hatch, H. M., Jiang, T., Morse, D. A., Fox, S. C. and Padua, M. B. (2015). Adrenal development in mice requires GATA4 and GATA6 transcription factors. *Endocrinology* **156**, 2503-2517. doi:10.1210/en.2014-1815

Thiesler, H., Beimdiek, J. and Hildebrandt, H. (2021). Polysialic acid and Siglec-E orchestrate negative feedback regulation of microglia activation. *Cell. Mol. Life Sci.* **78**, 1637-1653. doi:10.1007/s00018-020-03601-z

Tremblay, M., Sanchez-Ferras, O. and Bouchard, M. (2018). GATA transcription factors in development and disease. *Development* **145**, dev164384. doi:10.1242/dev.164384

Trowe, M.-O., Airik, R., Weiss, A.-C., Farin, H. F., Foik, A. B., Bettenhausen, E., Schuster-Gossler, K., Taketo, M. M. and Kispert, A. (2012). Canonical Wnt signaling regulates smooth muscle precursor development in the mouse ureter. *Development* **139**, 3099-3108. doi:10.1242/dev.077388

van Amerongen, R., Bowman, A. N. and Nusse, R. (2012). Developmental stage and time dictate the fate of Wnt/β-catenin-responsive stem cells in the mammary gland. *Cell Stem Cell* **11**, 387-400. doi:10.1016/j.stem.2012.05.023

van Tuyn, J., Knaän-Shanzer, S., van de Watering, M. J., de Graaf, M., van der Laarse, A., Schalij, M. J., van der Wall, E. E. and de Vries, A. A. (2005). Activation of cardiac and smooth muscle-specific genes in primary human cells after forced expression of human myocardin. *Cardiovasc. Res.* **67**, 245-255. doi:10.1016/j.cardiores.2005.04.013

Wada, H., Hasegawa, K., Morimoto, T., Kakita, T., Yanazume, T., Abe, M. and Sasayama, S. (2002). Calcineurin-GATA-6 pathway is involved in smooth muscle-specific transcription. *J. Cell Biol.* **156**, 983-991. doi:10.1083/jcb.200106057

Wang, D. Z. and Olson, E. N. (2004). Control of smooth muscle development by the myocardin family of transcriptional coactivators. *Curr. Opin. Genet. Dev.* **14**, 558-566. doi:10.1016/j.gde.2004.08.003

Wang, D., Chang, P. S., Wang, Z., Sutherland, L., Richardson, J. A., Small, E., Krieg, P. A. and Olson, E. N. (2001). Activation of cardiac gene expression by myocardin, a transcriptional cofactor for serum response factor. *Cell* **105**, 851-862. doi:10.1016/S0092-8674(01)00404-4

Wang, Z., Wang, D. Z., Pipes, G. C. and Olson, E. N. (2003). Myocardin is a master regulator of smooth muscle gene expression. *Proc. Natl. Acad. Sci. USA* **100**, 7129-7134. doi:10.1073/pnas.1232341100

Weiss, R. M., Guo, S., Shan, A., Shi, H., Romano, R.-A., Sinha, S., Cantley, L. G. and Guo, J.-K. (2013). Brg1 determines urothelial cell fate during ureter development. *J. Am. Soc. Nephrol.* **24**, 618-626. doi:10.1681/ASN.2012090902

Weiss, A.-C., Bohnenpoll, T., Kurz, J., Blank, P., Airik, R., Ludtke, T. H., Kleppa, M.-J., Deuper, L., Kaiser, M., Mamo, T. M. et al. (2019). Delayed onset of smooth muscle cell differentiation leads to hydroureter formation in mice with conditional loss of the zinc finger transcription factor gene Gata2 in the ureteric mesenchyme. *J. Pathol.* **248**, 452-463. doi:10.1002/path.5270

Werneburg, S., Buettner, F. F. R., Mühlenhoff, M. and Hildebrandt, H. (2015). Polysialic acid modification of the synaptic cell adhesion molecule SynCAM 1 in human embryonic stem cell-derived oligodendrocyte precursor cells. *Stem Cell Res.* **14**, 339-346. doi:10.1016/j.scr.2015.03.001

Whissell, G., Montagni, E., Martinelli, P., Hernando-Momblona, X., Sevillano, M., Jung, P., Cortina, C., Calon, A., Abuli, A., Castells, A. et al. (2014). The transcription factor GATA6 enables self-renewal of colon adenoma stem cells by repressing BMP gene expression. *Nat. Cell Biol.* **16**, 695-707. doi:10.1038/ncb2992

Wilkinson, D. G. and Nieto, M. A. (1993). Detection of messenger RNA by in situ hybridization to tissue sections and whole mounts. *Methods Enzymol.* **225**, 361-373. doi:10.1016/0076-6879(93)25025-W

Yin, F. and Herring, B. P. (2005). GATA-6 can act as a positive or negative regulator of smooth muscle-specific gene expression. *J. Biol. Chem.* **280**, 4745-4752. doi:10.1074/jbc.M411585200

Yu, J., Carroll, T. J. and McMahon, A. P. (2002). Sonic hedgehog regulates proliferation and differentiation of mesenchymal cells in the mouse metanephric kidney. *Development* **129**, 5301-5512. doi:10.1242/dev.129.22.5301

Yu, Z., Mannik, J., Soto, A., Lin, K. K. and Andersen, B. (2009). The epidermal differentiation-associated Grainyhead gene Get1/Grhl3 also regulates urothelial differentiation. *EMBO J.* **28**, 1890-1903. doi:10.1038/emboj.2009.142

Zeng, L. and Childs, S. J. (2012). The smooth muscle microRNA miR-145 regulates gut epithelial development via a paracrine mechanism. *Dev. Biol.* **367**, 178-186. doi:10.1016/j.ydbio.2012.05.009

Zhao, R., Watt, A. J., Li, J., Luebke-Wheeler, J., Morrisey, E. E. and Duncan, S. A. (2005). GATA6 is essential for embryonic development of the liver but dispensable for early heart formation. *Mol. Cell. Biol.* **25**, 2622-2631. doi:10.1128/MCB.25.7.2622-2631.2005

Zhao, R., Watt, A. J., Battle, M. A., Li, J., Bondow, B. J. and Duncan, S. A. (2008). Loss of both GATA4 and GATA6 blocks cardiac myocyte differentiation and results in acardia in mice. *Dev. Biol.* **317**, 614-619. doi:10.1016/j.ydbio.2008.03.013

Zimmerman, L. B., De Jesús-Escobar, J. M. and Harland, R. M. (1996). The Spemann organizer signal noggin binds and inactivates bone morphogenetic protein 4. *Cell* **86**, 599-606. doi:10.1016/S0092-8674(00)80133-6

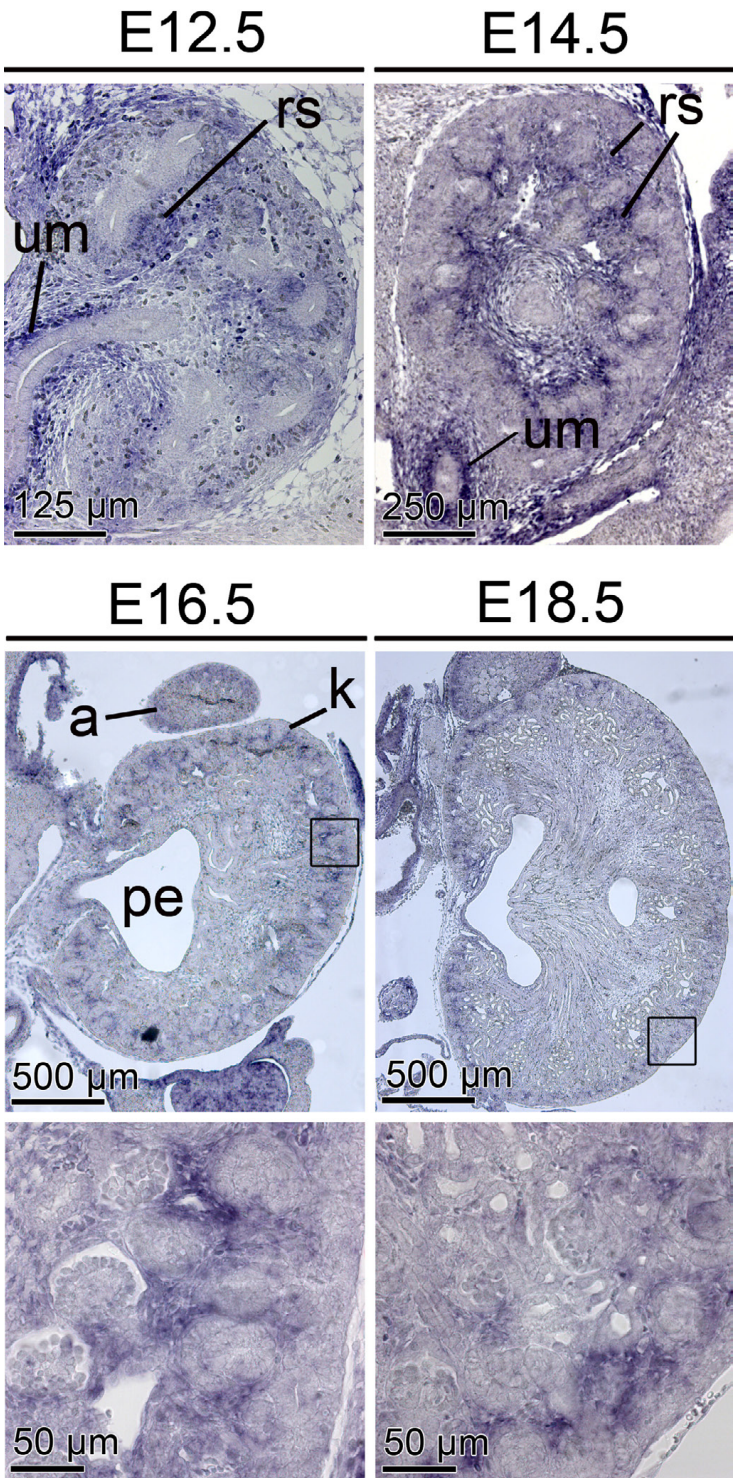

Fig. S1. *Gata6* expression occurs in the renal stroma. *In situ* hybridization analysis of *Gata6* expression on sagittal kidney sections of E12.5, E14.5, E16.5 and E18.5 wildtype embryos. Note that *Gata6* expression occurs in the entire renal stroma at E12.5 and E14.5, but is confined to the stroma at the medullary-cortical border region at E16.5 and E18.5. n≥3 for each stage. a, adrenal gland; k, kidney; pe, renal pelvis; rs, renal stroma; um, ureteric mesenchyme.

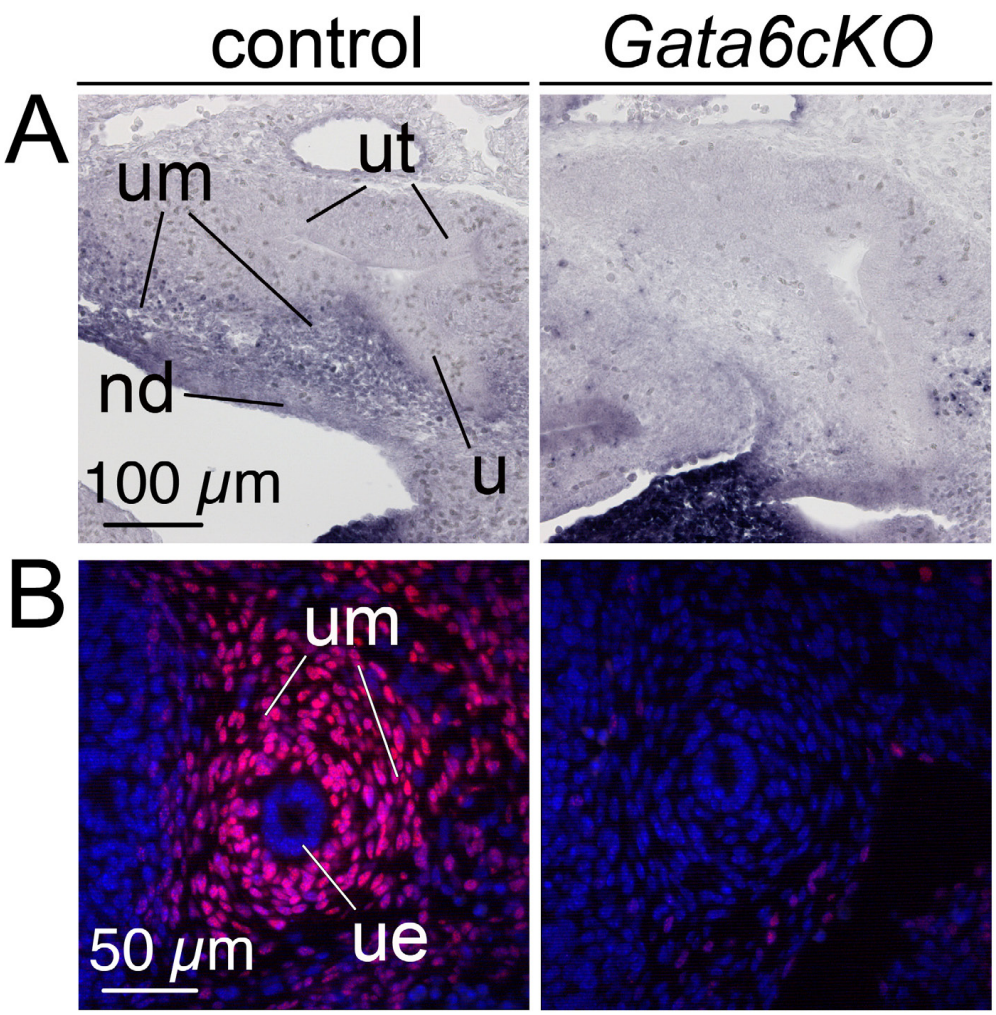

Fig. S2. The *Tbx18*^{cre} driver line mediates conditional deletion of *Gata6* in the UM. (A) *In situ* hybridization analysis of *Gata6* expression on sagittal sections of the metanephros of E11.5 wildtype and *Gata6cKO* (*Tbx18*$^{cre/+}$;*Gata6*$^{fl/fl}$) embryos using a probe against exon2, which is floxed in the *Gata6*^{fl} allele. (B) Immunofluorescence analysis of GATA6 protein on proximal sections of the ureter at E12.5. n≥3 for each assay and genotype. nd, nephric duct; ue, ureteric epithelium; um, ureteric mesenchyme; ut, ureteric tip; u, ureter.

A

Genotype	*Tbx18*$^{+/+}$; *Gata6*$^{fl/+}$	*Tbx18*$^{+/+}$; *Gata6*$^{fl/fl}$	*Tbx18*$^{cre/+}$; *Gata6*$^{fl/+}$	*Tbx18*$^{cre/+}$; *Gata6*$^{fl/fl}$
(expected %)	(25%)	(25%)	(25%)	(25%)
E11.5, n=94	26 (28%)	25 (27%)	21 (22%)	22 (23%)
E12.5, n=896	220 (25%)	206 (23%)	251 (28%)	219 (24%)
E14.5, n=575	132 (23%)	139 (24%)	151 (26%)	153 (27%)
E15.5, n=95	31 (33%)	19 (20%)	19 (20%)	26 (27%)
E16.5, n=102	33 (32%)	22 (22%)	24 (23%)	23 (23%)
E18.5, n=205	57 (28%)	45 (22%)	48 (23%)	55 (27%)

B

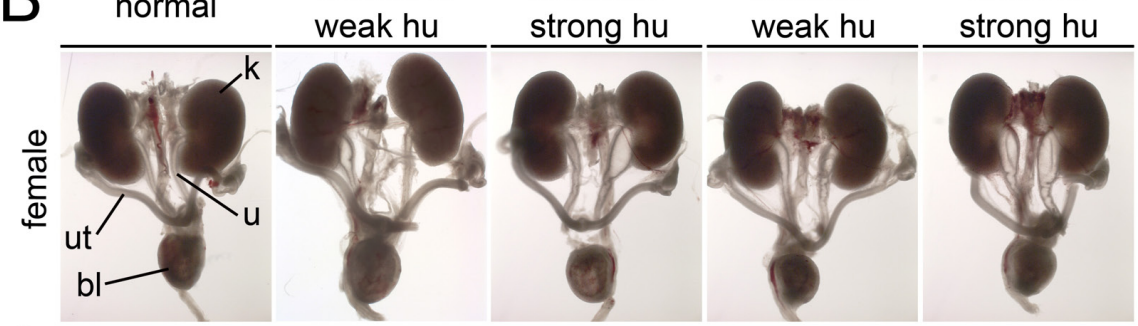

C

Genotype female	Control	*Tbx18*$^{cre/+}$; *Gata6*$^{fl/+}$	*Tbx18*$^{cre/+}$; *Gata6*$^{fl/fl}$
normal	26 (93%)	3 (25%)	5 (19%)
unilateral weak hu	1 (3.5%)	2 (17%)	4 (15%)
unilateral strong hu	0	2 (17%)	2 (8%)
bilateral weak hu	1 (3.5%)	5 (42%)	7 (27%)
bilateral strong hu	0	0	8 (31%)
total number	28	12	26

D

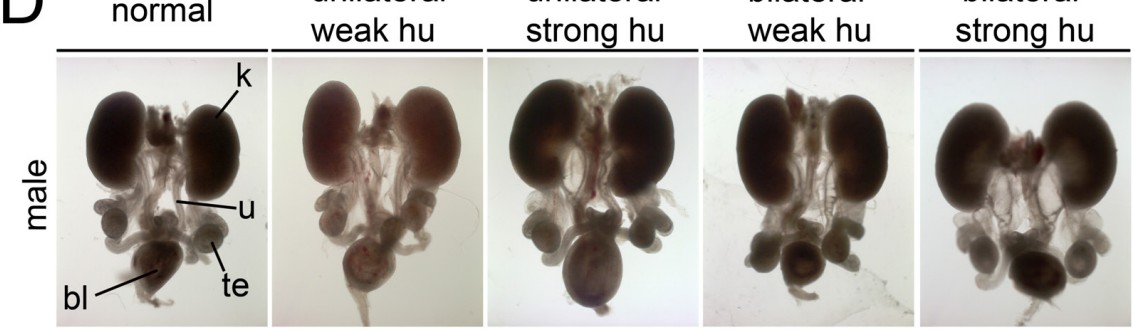

E

Genotype male	Control	*Tbx18*$^{cre/+}$; *Gata6*$^{fl/+}$	*Tbx18*$^{cre/+}$; *Gata6*$^{fl/fl}$
normal	33 (89%)	6 (30%)	5 (22%)
unilateral weak hu	3 (8%)	7 (35%)	3 (13%)
unilateral strong hu	0	1 (5%)	2 (9%)
bilateral weak hu	1 (3%)	6 (30%)	8 (35%)
bilateral strong hu	0	0	5 (22%)
total number	37	20	23

Fig. S3.

Fig. S3. *Gata6cKO* embryos are viable and display ureter dilatation of variable severity at E18.5. (A) Distribution of genotypes in litters of matings of *Tbx18*$^{cre/+}$;*Gata6*$^{fl/+}$ males with *Gata6*$^{fl/fl}$ females at the indicated stages. Shown are the stages, the number of embryos, the expected and obtained frequency of the indicated genotypes. (B) Morphology of whole urogenital systems of E18.5 female *Gata6cKO* embryos displaying different grades of hydroureter (hu) used for classification in the Table shown in (C). (C) Distribution of ureter dilatations of different severity in female *Tbx18*$^{cre/+}$;*Gata6*$^{fl/+}$ and *Tbx18*$^{cre/+}$;*Gata6*$^{fl/fl}$ embryos at E18.5. (D) Morphology of whole urogenital systems of E18.5 male *Gata6cKO* embryos displaying different grades of hydroureter (hu) used for classification in the Table shown in (E). (E) Distribution of ureter dilatations of different severity in male *Tbx18*$^{cre/+}$;*Gata6*$^{fl/+}$ and *Tbx18*$^{cre/+}$;*Gata6*$^{fl/fl}$ embryos at E18.5. bl, bladder; k, kidney; te, testis; u, ureter; ut, uterus.

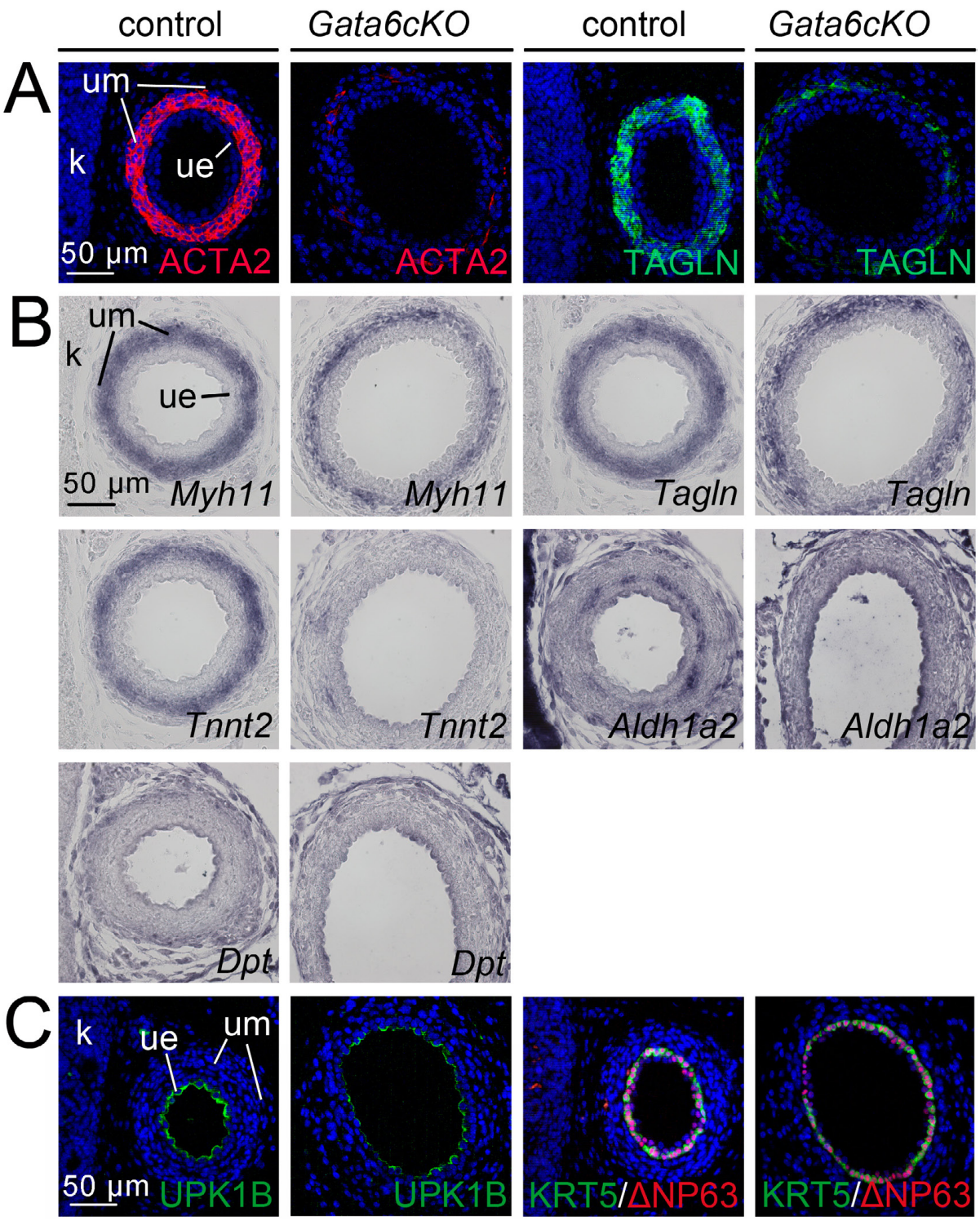

Fig. S4. Weak proximal hydroureter is associated with reduced expression of SMC markers in *Gata6cKO* embryos at E18.5. (A) Immunofluorescence of the SMC markers ACTA2 and TAGLN and (B) RNA *in situ* hybridization analysis of SMC genes (*Tagln, Tnnt2, Myh11*), of the *lamina propria* marker *Aldh1a2*, and of the *tunica adventitia* marker *Dpt* on transverse sections of the proximal ureter. (C) Analysis of urothelial differentiation by immunofluorescent detection of the B-cell marker KRT5, the I/B-cell marker ΔNP63 and the S-cell marker UPK1B on proximal ureter sections. Nuclei are counterstained with DAPI (blue, in A and C). n≥3 for each assay, genotype and probe. k, kidney; ue, ureteric epithelium; um, ureteric mesenchyme.

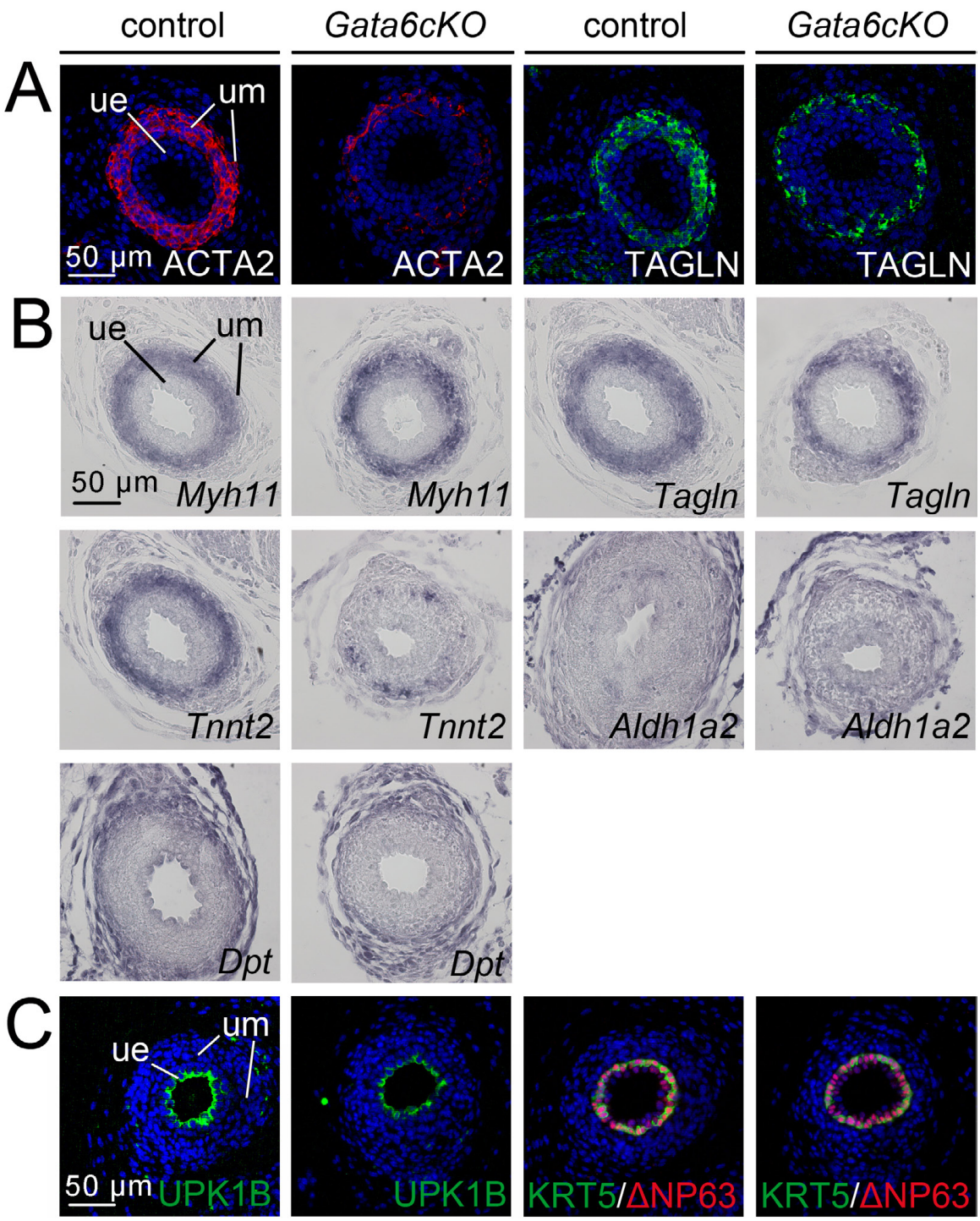

Fig. S5. Expression of SMC markers is partly reduced in distal ureters in *Gata6cKO* embryos at E18.5. (A) Immunofluorescence of the SMC markers ACTA2 and TAGLN and (B) RNA *in situ* hybridization analysis of SMC genes (*Tagln, Tnnt2, Myh11*), of the *lamina propria* marker *Aldh1a2*, and of the *tunica adventitia* marker *Dpt* on transverse sections of the proximal ureter. (C) Analysis of urothelial differentiation by immunofluorescent detection of the B-cell marker KRT5, the I/B-cell marker ΔNP63 and the S-cell marker UPK1B on proximal ureter sections. Nuclei are counterstained with DAPI (blue, in A and C). n≥3 for each assay, genotype and probe. ue, ureteric epithelium; um, ureteric mesenchyme.

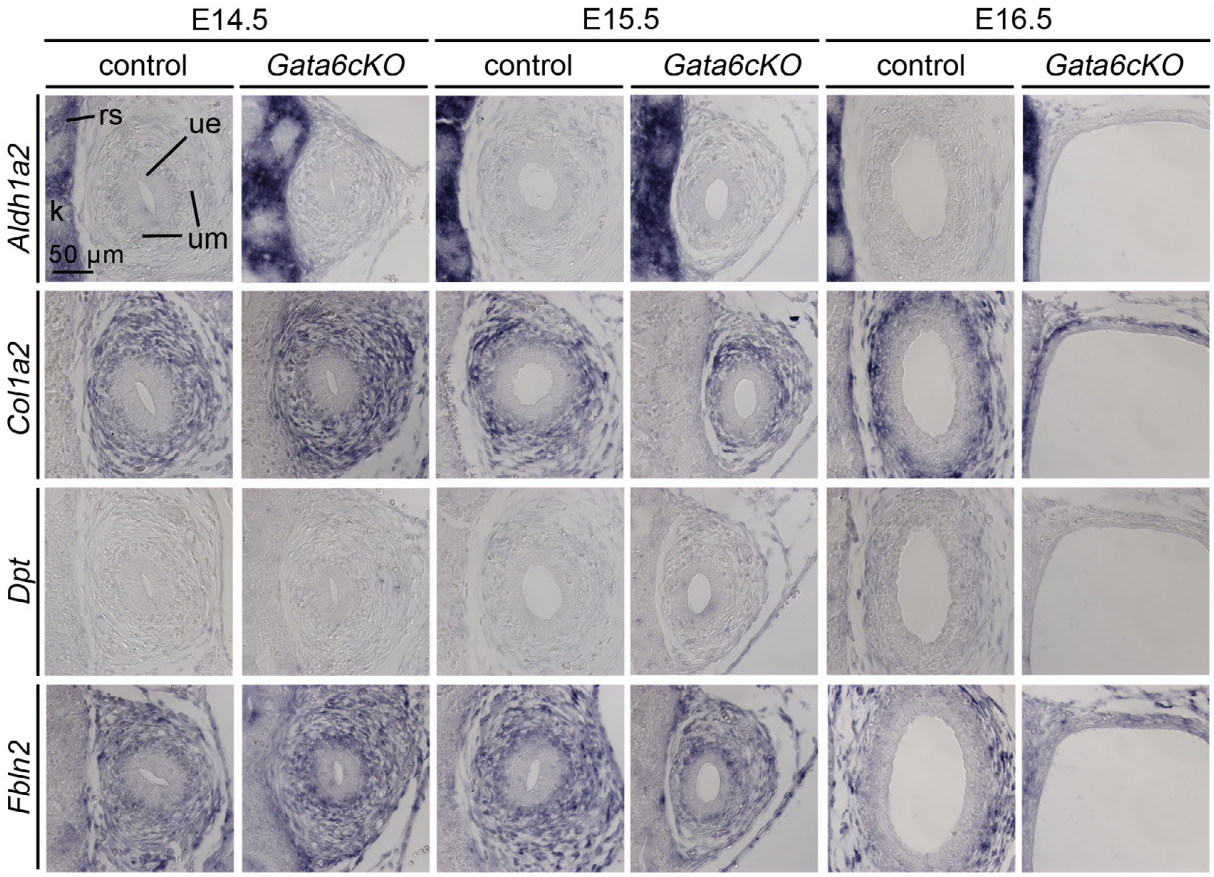

Fig. S6. Differentiation of fibrocytes is unchanged in *Gata6cKO* ureters at E14.5 to E16.5. Shown are RNA *in situ* hybridization analyses on sections of the proximal ureter at E14.5, E15.5 and E16.5 of control and *Gata6cKO* embryos for the *lamina propria* marker *Aldh1a2* and the *tunica adventitia* markers *Col1a2, Dpt, Fbln2*. n≥3 for each probe, stage and genotype. k, kidney; rs, renal stroma; ue, ureteric epithelium; um, ureteric mesenchyme.

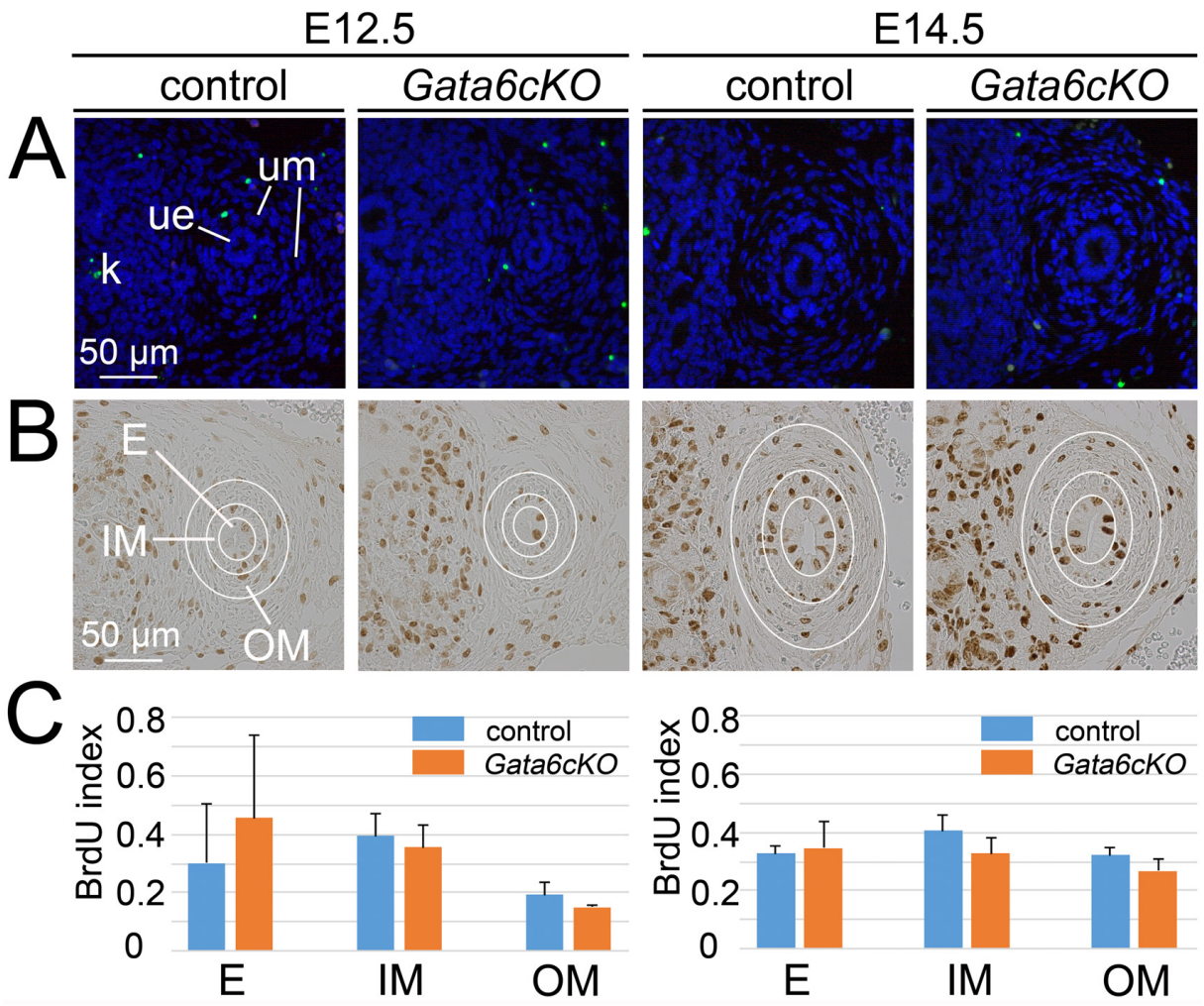

Fig. S7. Proliferation and apoptosis are not affected in *Gata6cKO* ureters at E12.5 and E14.5. (A) Immunofluorescent analysis of apoptosis (green) by the TUNEL assay on proximal ureter sections. Nuclei are counterstained with DAPI (blue). k, kidney; ue, ureteric epithelium; um, ureteric mesenchyme. (B) Immunohistochemical detection of BrdU on proximal ureter sections. White circles demarcate the ureteric epithelium (E), the inner and outer mesenchymal cell populations (IM and OM). n=3, each assay and stage. (C) Quantification of BrdU-positive cells in E12.5 control (n=3) versus mutant (n=3) ureters. Values are displayed as mean ± sd. All values are ns, *i.e.* P>0.05; two-tailed Student's t-test. For source data and statistics see Table S1.

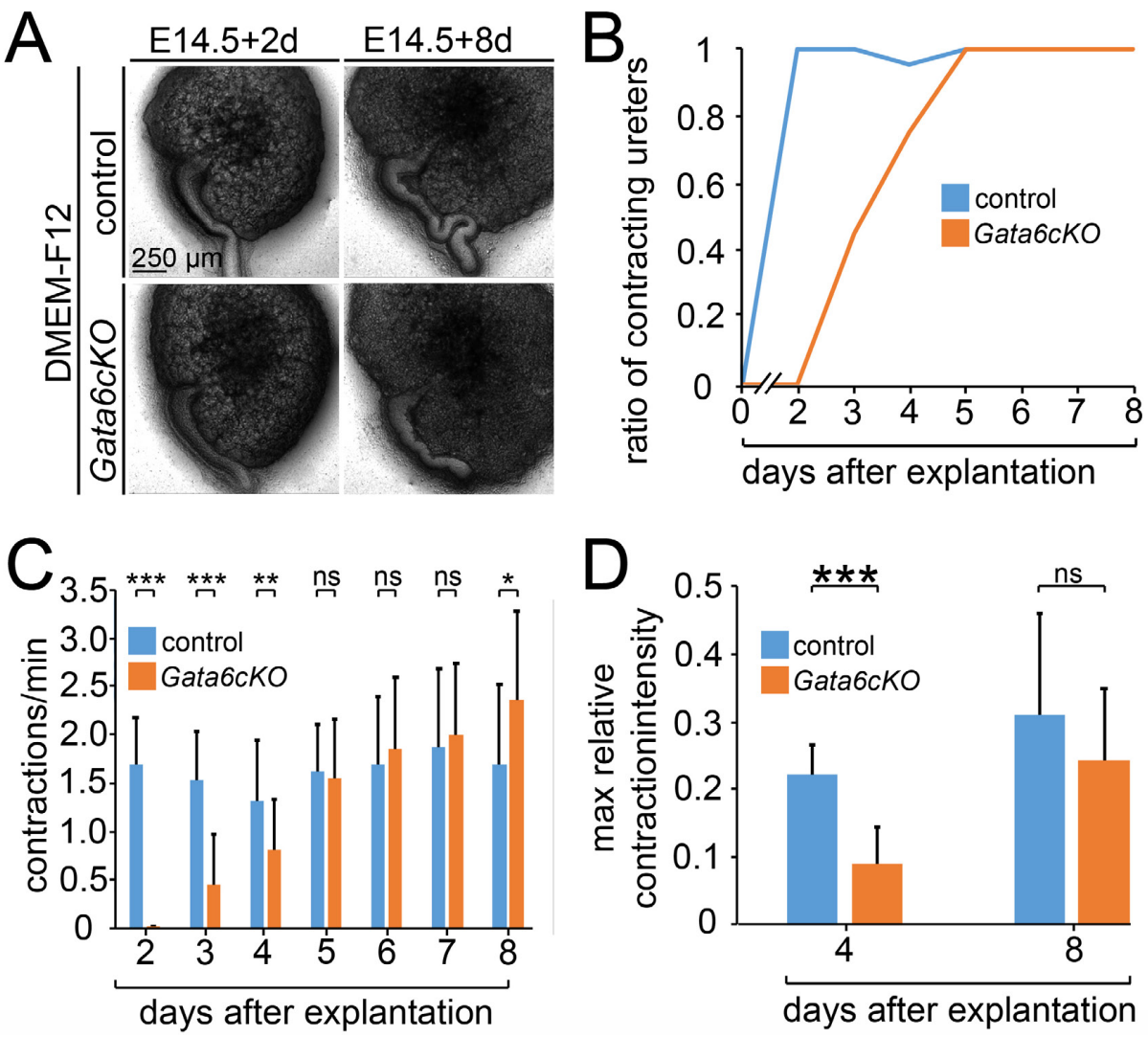

Fig. S8. Peristaltic activity is regained *in Gata6cKO* ureters in serum-free cultures. (A) E14.5 combined ureters and kidneys were explanted and grown for 8 days in culture with minimal medium, i.e. without FCS. Morphology and peristaltic activity were monitored every day from day 2 onwards using video-microscopy. (B) The onset of contraction was delayed by 2 to 3 days in *Gata6cKO* ureters (n=20) compared to control ureters (n=23). (C) Statistical analysis of peristaltic activity (expressed as contractions per min) of control (n=23) and mutant ureters (n=20). Bar graphs display mean±sd. Differences were considered significant with a P-value below 0.05 ($p<0.05$, *), highly significant ($p\leq0.005$, **) and extremely significant ($p\leq 0.0005$, ***), two-tailed Student's *t*-test. For source data and statistics see Table S4. (D) Contraction intensity was reduced after 4 days in culture in *Gata6cKO* mutants (n=15) compared to the control (n=22) but caught up after 8 days in culture (control n=23, *Gata6cKO* n=20). Bar graphs display mean±sd. Significance levels are as in (C). For source data and statistics see Table S4.

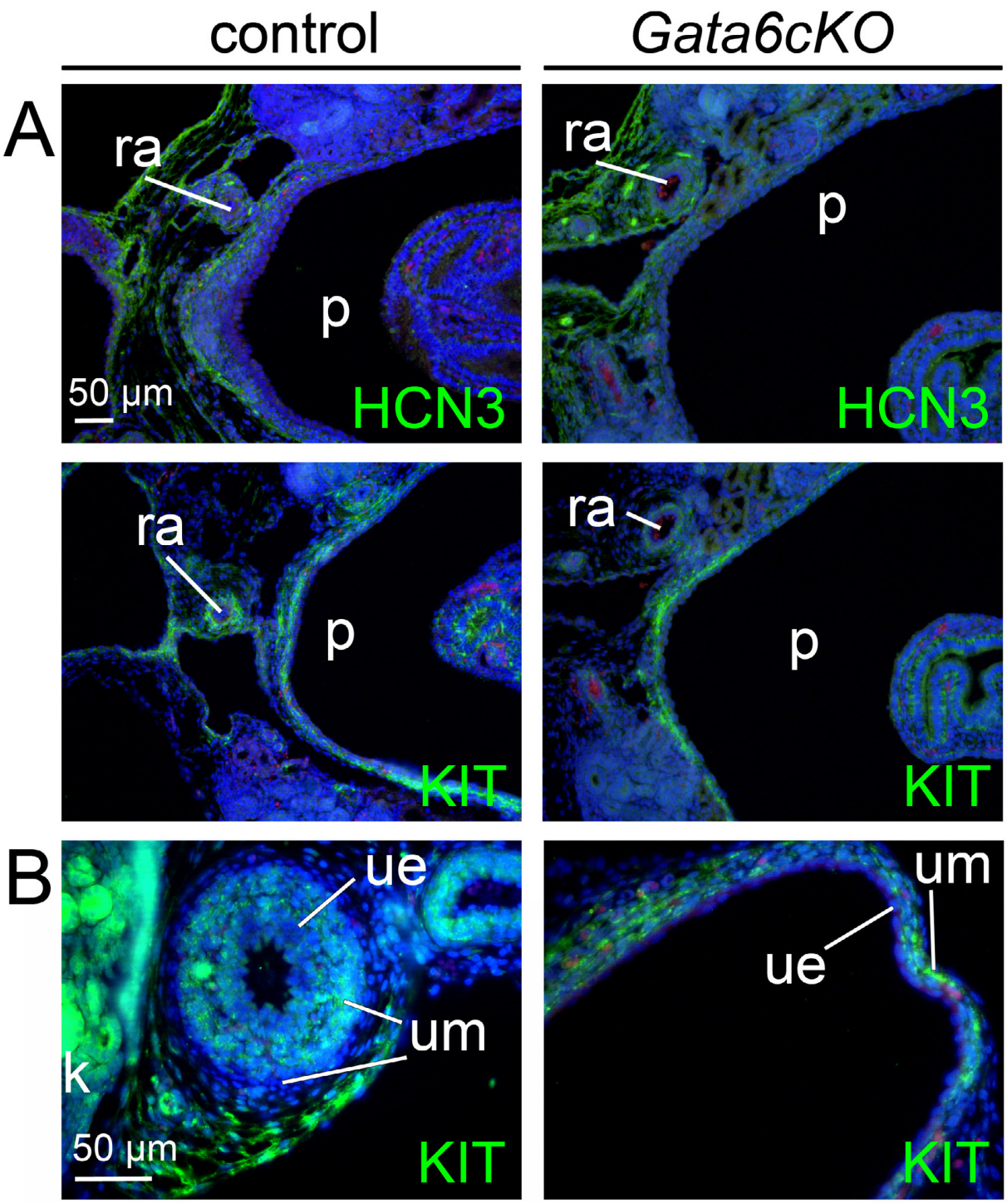

Fig. S9. Loss of *Gata6* in the UM does not affect the excitation/conduction system of the upper urinary tract. Immunofluorescence analysis of sagittal kidney (A) and proximal ureter sections (B) of E18.5 control and *Gata6cKO* embryos. Expression of HCN3, a marker for the pacemaker cells in the renal pelvis, and of KIT, a marker for interstitial Cajal-like cells in the renal pelvis and the mesenchymal region of the ureter is unchanged. k, kidney; p, pelvis; ra, renal artery; ue, ureteric epithelium; um, ureteric mesenchyme.

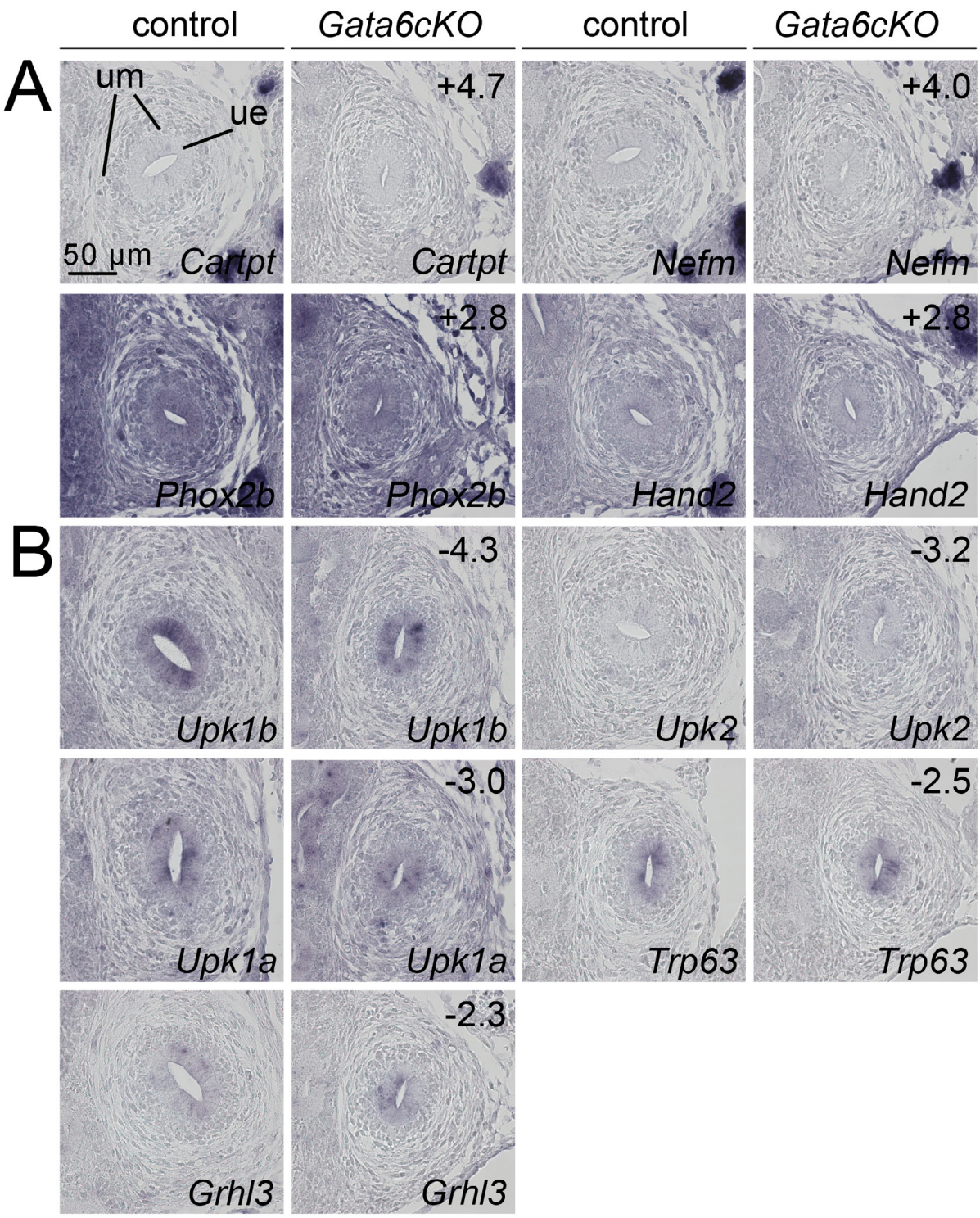

Fig. S10. RNA *in situ* hybridization analysis of genes with altered expression in microarrays of E14.5 *Gata6cKO* ureters. (A,B) Shown are RNA *in situ* hybridization analyses of proximal ureter sections of control and *Gata6cKO* embryos for genes with increased expression (A) and genes with decreased expression (B) in *Gata6cKO* microarrays. Probes, genotypes and fold changes in the microarray are as indicated. n≥3 for each probe and genotype. ue, ureteric epithelium; um, ureteric mesenchyme.

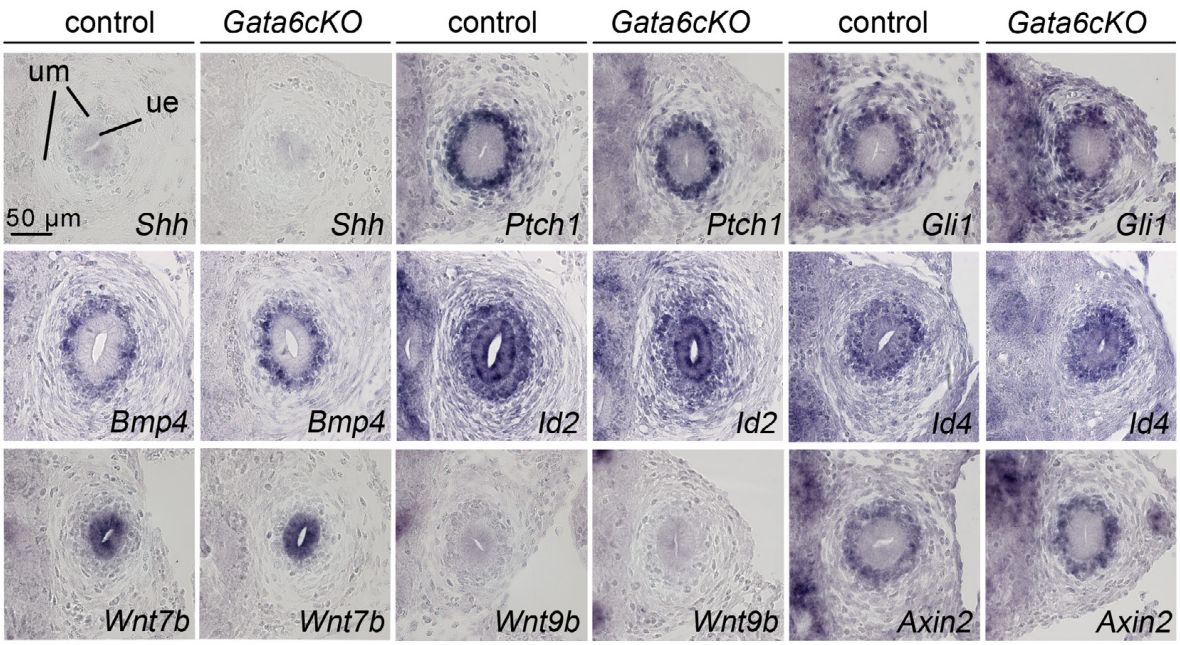

Fig. S11. Signaling pathways relevant for SMC differentiation are unchanged in their activity/expression in *Gata6cKO* ureters at E14.5. Shown are RNA *in situ* hybridization analyses on sections of the proximal ureter of E14.5 control and *Gata6cKO* embryos of *Shh*, and the targets of SHH signaling, *Ptch1* and *Gli1*; of *Wnt7b* and *Wnt9b, a*nd the WNT target gene *Axin2;* of *Bmp4,* and its target genes *Id2* and *Id4*. n≥3 for each probe and genotype. ue, ureteric epithelium; um, ureteric mesenchyme.

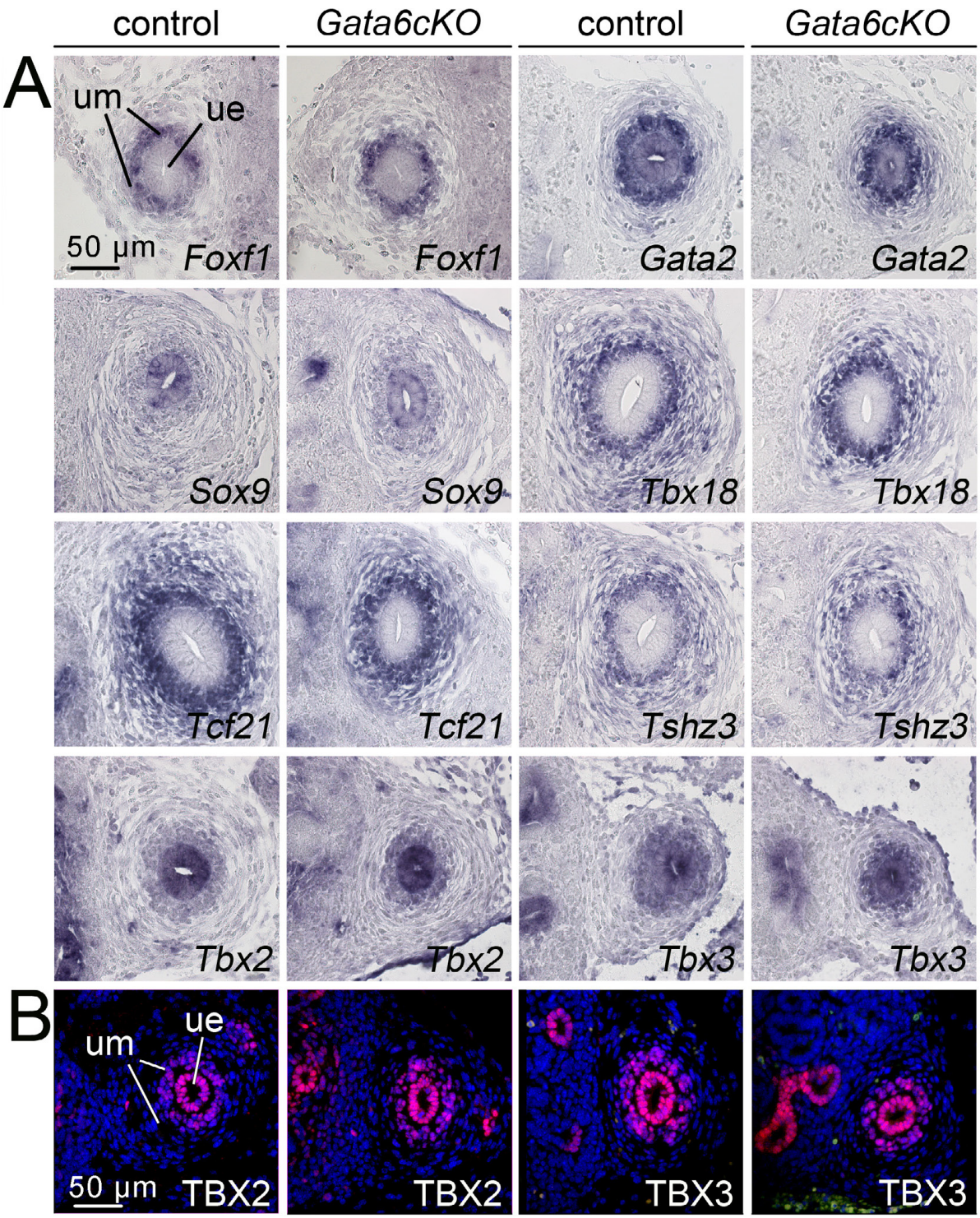

Fig. S12. Transcription factors relevant for SMC differentiation are unchanged in their expression in *Gata6cKO* ureters at E14.5. (A) RNA *in situ* hybridization analysis for expression of *Foxf1*, *Gata2, Sox9, Tbx18*, *Tcf21, Tshz3*, *Tbx2*, *Tbx3* and (B) immunofluorescence analysis of TBX2 and TBX3 on sections of the proximal ureter at E14.5 of control and *Gata6cKO* embryos. Nuclei are counterstained with DAPI (B). n>=3, each probe, assay and genotype. ue, ureteric epithelium; um, ureteric mesenchyme.

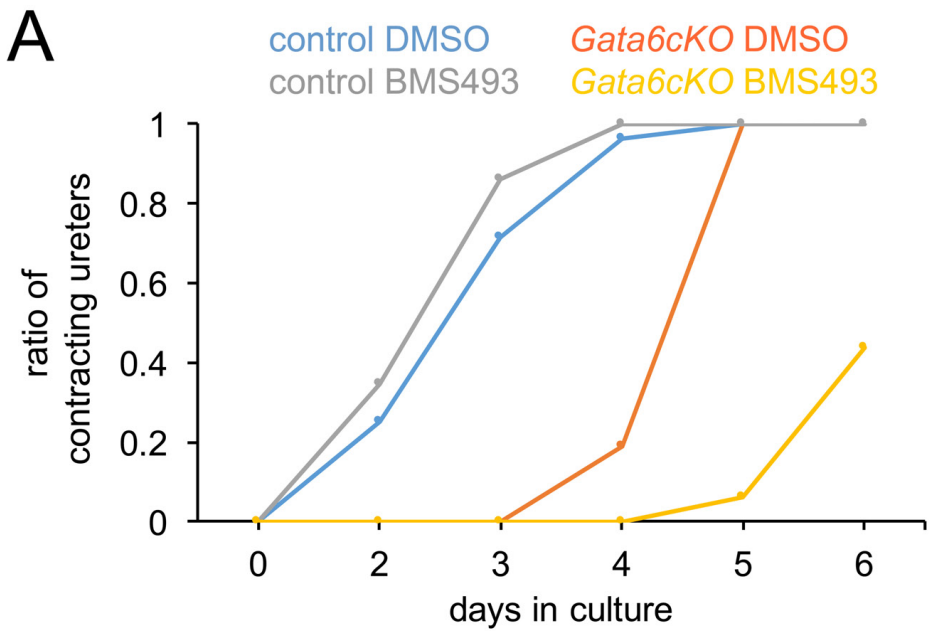

B

days in culture	2	3	4	5	6
control DMSO vs. Gata6cKO DMSO	ns	***	***	***	*
control BMS493 vs. Gata6cKO BMS493	*	***	***	***	***
control DMSO vs.control BMS493	ns	ns	***	***	***
Gata6cKO DMSO vs. Gata6cKO BMS493			ns	***	***

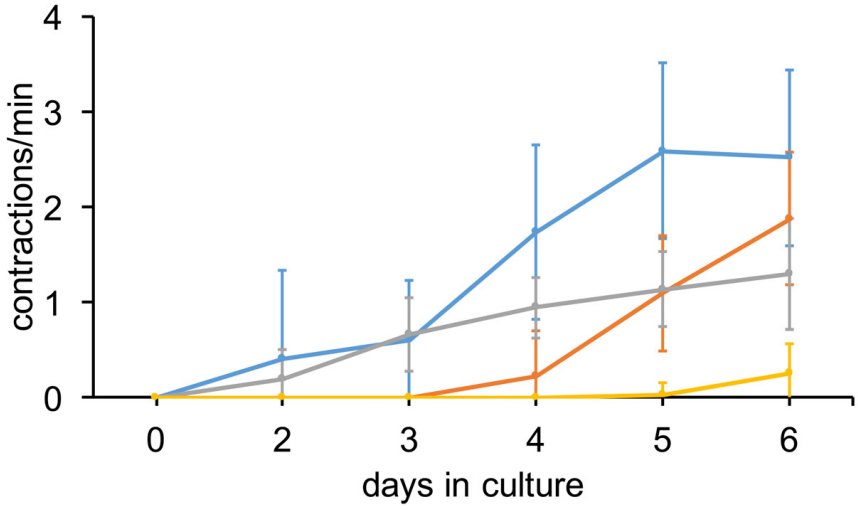

Fig. S13. Reduction of RA signaling does not rescue peristalsis defects in *Gata6cKO* ureters. Kidney rudiments from E13.5 control and *Gata6cKO* embryos were explanted and cultured for 6 days in the presence of DMSO (control) or 1 µM of the RA signaling inhibitor BMS493. Peristalsis was monitored daily in 1-min intervals. (A) Percentage of ureters that show peristaltic activity at the individual days during the culture period. (B) Statistical analysis of peristaltic activity (expressed as contractions per min) of control DMSO-treated (n=28), control BMS493-treated (n=29), mutant DMSO-treated (n=16) and mutant BMS493-treated (n=16) ureters. Bar graphs display mean±sd. Differences were considered significant with a P-value below 0.05 ($p<0.05$, *), highly significant ($p\leq0.005$, **) and extremely significant ($p\leq 0.0005$, ***); two-tailed Student's *t*-test. For source data and statistics see Table S12.

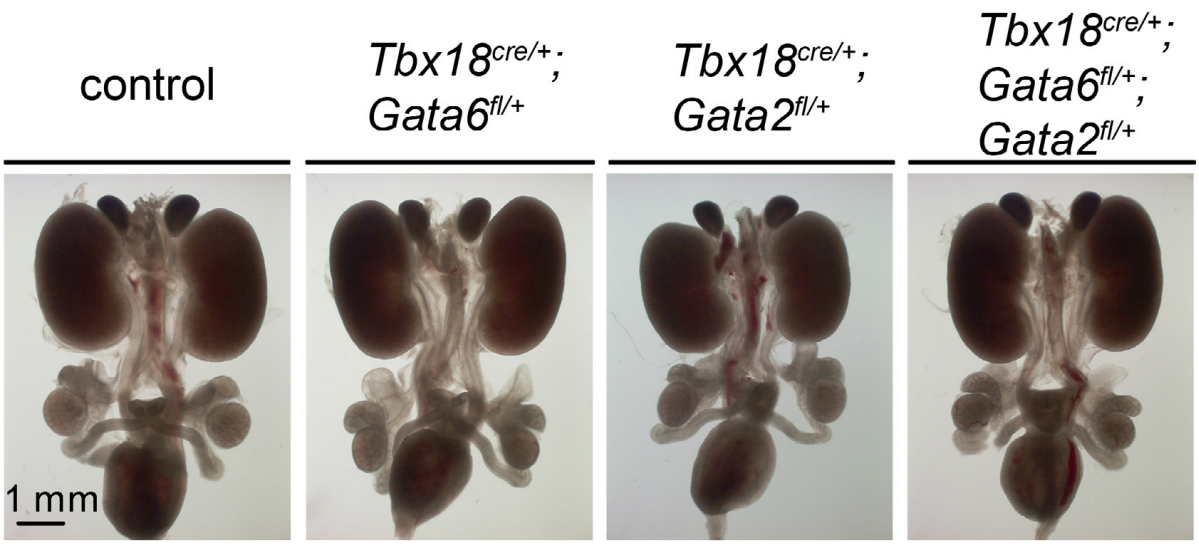

Fig. S14. *Gata2* and *Gata6* do not genetically interact in SMC differentiation in the developing ureter. Morphological analysis of whole urogenital systems of control (n=20), *Tbx18*$^{cre/+}$;*Gata6*$^{fl/+}$ (n=14), *Tbx18*$^{cre/+}$;*Gata2*$^{fl/+}$ (n=3) and *Tbx18*$^{cre/+}$;*Gata6*$^{fl/+}$;*Gata2*$^{fl/+}$(n=20) embryos at E18.5.

Table S1. Statistical evaluation of the BrdU incorporation assay in E12.5 and E14.5 control and Gata6cKO ureters.

Click here to download Table S1

Table S2. Statistics of the peristaltic frequency of explant cultures of E14.5 control and Gata6cKO ureters.

Click here to download Table S2

Table S3. Statistics of the peristaltic intensity of explant cultures of E14.5 control and Gata6cKO ureters.

Click here to download Table S3

Table S4. Statistics on the peristaltic activity of explants of E14.5 Gata6cKO ureters cultured together with kidneys for 8 days in DMEM-F12-only medium (relates to Fig. S8).

Click here to download Table S4

Table S5. Statistics of the peristaltic frequency of explant cultures of E18.5 control and Gata6cKO ureters.

Click here to download Table S5

Table S6. Statistics of the peristaltic intensity of explant cultures of E18.5 control and Gata6cKO ureters.

Click here to download Table S6

Table S7. Genes with increased expression in microarrays of E14.5 Gata6cKO ureters.

Click here to download Table S7

Table S8. Genes with decreased expression in microarrays of E14.5 Gata6cKO ureters.

Click here to download Table S8

Table S9. Functional annotation by DAVID for genes with increased expression in the microarray of E14.5 Gata6cKO ureters.

Click here to download Table S9

Table S10. Functional annotation by DAVID for genes with decreased expression in the microarray of E14.5 Gata6cKO ureters.

Click here to download Table S10

Table S11. RT-qPCR analysis of SMC gene expression in control and Gata6cKO ureters at E14.5.

Click here to download Table S11

Table S12. Statistics of the peristaltic frequency of explant cultures of E18.5 control and Gata6cKO ureters treated with the pan-RAR antagonist BMS493.

Click here to download Table S12

Table S13. GATA6 and FOXF1 cooperate in Myocd activation in NIH3T3 cells (relates to Figure 7A).

Click here to download Table S13

Table S14. Statistical analysis of peristaltic activity of ureters with misexpression of Foxf1 (relates to Figure 7B).

Click here to download Table S14

Table S15. Primers for RT-qPCR analysis of gene expression.

Click here to download Table S15